Prepared in cooperation with the Alabama Power Company

Erosion Monitoring Along Selected Bank Locations of the Coosa River in Alabama Using Terrestrial Light Detection and Ranging (T–Lidar) Technology, 2014–17

Scientific Investigations Report 2019–5023

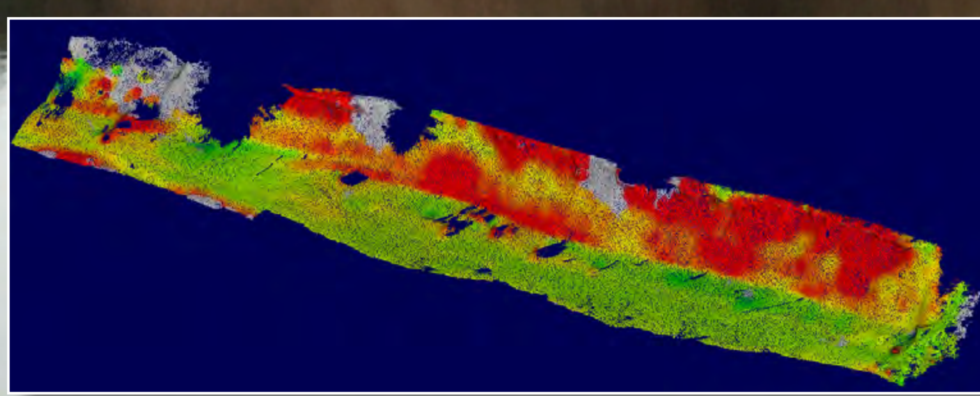

U.S. Department of the Interior
U.S. Geological Survey

Cover. Logan Martin Dam site LM–102 on the Coosa River near Vincent, Alabama, as viewed from upstream mid-channel during the survey on October 30, 2015. Inset: Difference between surveyed surfaces at Logan Martin Dam site LM–102 on the Coosa River near Vincent, Alabama, for the period October 16, 2014, through July 18, 2017.

Back cover. H. Neely Henry Dam site NH–109 on the Coosa River near Gadsden, Alabama, as viewed from downstream mid-channel during the survey on June 23, 2015. Inset: Difference between surveyed surfaces at Neely Henry Dam site NH–108 on the Coosa River near Gadsden, Alabama, for the period January 30, 2015, through July 19, 2017.

Photographs by Kathryn G. Lee, U.S. Geological Survey.

Erosion Monitoring Along Selected Bank Locations of the Coosa River in Alabama Using Terrestrial Light Detection and Ranging (T–Lidar) Technology, 2014–17

By Richard J. Huizinga and Daniel M. Wagner

Prepared in cooperation with the Alabama Power Company

Scientific Investigations Report 2019–5023

U.S. Department of the Interior
U.S. Geological Survey

U.S. Department of the Interior
DAVID BERNHARDT, Acting Secretary

U.S. Geological Survey
James F. Reilly II, Director

U.S. Geological Survey, Reston, Virginia: 2019

For more information on the USGS—the Federal source for science about the Earth, its natural and living resources, natural hazards, and the environment—visit https://www.usgs.gov or call 1–888–ASK–USGS.

For an overview of USGS information products, including maps, imagery, and publications, visit https://store.usgs.gov.

Suggested citation:
Huizinga, R.J., and Wagner, D.M., 2019, Erosion monitoring along selected bank locations of the Coosa River in Alabama using terrestrial light detection and ranging (T–lidar) technology, 2014–17: U.S. Geological Survey Scientific Investigations Report 2019–5023, 28 p., https://doi.org/10.3133/sir20195023.

ISSN 2328-0328 (online)

Acknowledgments

The authors would like to express their appreciation to our former U.S. Geological Survey colleagues, Kathryn Lee and William Moody, who were instrumental in starting the project and collected data for the first 2 years of the study described herein. Additionally, U.S. Geological Survey field technician Andrew Vanover was very helpful in subsequent data collection efforts.

The authors also appreciate the direct assistance of Keith Chandler from the Alabama Power Company for hourly flow data from the dams on the Coosa River.

Contents

Figures

Tables

Conversion Factors

U.S. customary units to International System of Units

Multiply	By	To obtain
	Length	
meter (m)	3.281	foot (ft)
meter (m)	1.094	yard (yd)
kilometer (km)	0.6214	mile (mi)
	Volume	
cubic meter (m^3)	1.308	cubic yard (yd^3)
	Flow rate	
cubic meter per second (m^3/s)	35.31	cubic foot per second (ft^3/s)

Datum

Vertical coordinate information is referenced to the North American Vertical Datum of 1988 (NAVD 88).

Horizontal coordinate information is referenced to the North American Datum of 1983 (NAD 83).

Supplemental Information

In this report, the words “left” and “right” generally refer to directions that would be reported by an observer facing downstream.

Normalized erosion is given in cubic meters per square meter (m^3/m^2).

Abbreviations

°	degree
ER	Enhanced Range
FOV	field of view
GNSS	Global Navigation Satellite System
HD	High Density
IMU	inertial measurement unit
INS	inertial navigation system
M3C2	Multiscale Model-to-Model Cloud Comparison
MC–lidar	motion-compensated light detection and ranging
MMS	Mobile Mapping Suite
OPUS	online positioning user service
POS-MV	Position and Orientation Solution for Marine Vessels
PPK	postprocessed kinematic (a type of differential correction for navigation with GNSS)
ROI	region of interest
SBET	smoothed best estimate of trajectory
TIN	triangulated irregular network
T–lidar	terrestrial light detection and ranging

Erosion Monitoring Along Selected Bank Locations of the Coosa River in Alabama Using Terrestrial Light Detection and Ranging (T–Lidar) Technology, 2014–17

By Richard J. Huizinga and Daniel M. Wagner

Abstract

The Alabama Power Company operates a series of dams on the Coosa River in east central Alabama. Seven dams impound the river to form six reservoirs: Weiss Lake, H Neely Henry Lake, Logan Martin Lake, Lay Lake, Lake Mitchell, and Lake Jordan. Streamflow below these reservoirs is primarily controlled by power generation at the dams, and there is ongoing concern about the stability of selected stream banks downstream from the dams. During relicensing in the early 2000s, the Alabama Power Company and stakeholders identified particular areas of concern to monitor and document the extent of erosion. The U.S. Geological Survey, in cooperation with the Alabama Power Company, conducted a 3-year monitoring program, from 2014 to 2017, of the geomorphic conditions of six selected reaches along the Coosa River. The six reaches included two downstream from H Neely Henry Dam near Gadsden, two downstream from Logan Martin Dam near Vincent, and two downstream from Walter Bouldin Dam near Wetumpka, Alabama. The geomorphic monitoring was conducted using boat- and tripod-mounted terrestrial light detection and ranging technology. Site LM–108, an island in the Coosa River downstream from Logan Martin Dam, exhibited the greatest amount of normalized erosion, 2.05 cubic meters per square meter of area, likely because this site experiences head-on flow from the river. Bank retreat at the upstream end of the island (LM–108) was estimated at 2.9 meters for the study period. The remaining five reaches were exposed to shear flow from the river; the greatest amount of normalized erosion, 0.467 cubic meter per square meter of area, was exhibited by site WB–106 on the right bank downstream from Walter Bouldin Dam. Results of the comparisons of terrestrial light detection and ranging scans indicated that intervals between scans that exhibited the greatest amounts of erosion generally corresponded to periods of above-median flow, and that intervals between scans that exhibited the least amounts of erosion, or deposition, generally corresponded to periods of below-median flow. Relatively smaller surface areas could be surveyed at some sites because inundation or dense vegetation obscured parts of the banks, suggesting that, in future investigations, it may be preferable to conduct scans during periods of leaf-off and low flow to avoid bias introduced by parts of the banks of interest being inundated or obscured by vegetation.

Introduction

The Alabama Power Company operates a series of dams on the Coosa River (fig. 1) in east-central Alabama. Seven dams impound the river to form six reservoirs: Weiss Lake, H Neely Henry Lake, Logan Martin Lake, Lay Lake, Lake Mitchell, and Lake Jordan. Two dams are associated with Lake Jordan: Jordan Dam, which is on the Coosa River, and Walter Bouldin Dam, which is on a diversion channel from Lake Jordan to the Coosa River downstream from Jordan Dam. These seven dams provide power generation, flood control, recreation, economic opportunity, and fish and wildlife habitats to the region.

Discharges below these reservoirs are primarily controlled by power generation at the dams, and there has been an ongoing concern about the stability of selected stream banks downstream from the dams (Kimbrow and Lee, 2013). As part of Federal Energy Regulatory Commission relicensure of the Coosa River project in the early 2000s, the Alabama Power Company and various stakeholders identified particular areas of concern and wanted to take steps to monitor and document the extent of erosion. The U.S. Geological Survey, in cooperation with the Alabama Power Company, conducted a monitoring program of the geomorphic conditions of selected reaches along the Coosa River downstream from H Neely Henry Dam near Gadsden, Logan Martin Dam near Vincent, and Walter Bouldin Dam near Wetumpka, Alabama. Boat- and tripod-mounted terrestrial light detection and ranging (T–lidar) technology was used to determine the condition of the bank at each study area. The results of this investigation serve as a valuable tool for the Alabama Power Company in evaluating any effects on the stream channel geomorphology.

T–lidar technology has proven to be well suited for erosion and mass-failure studies where conventional surveying

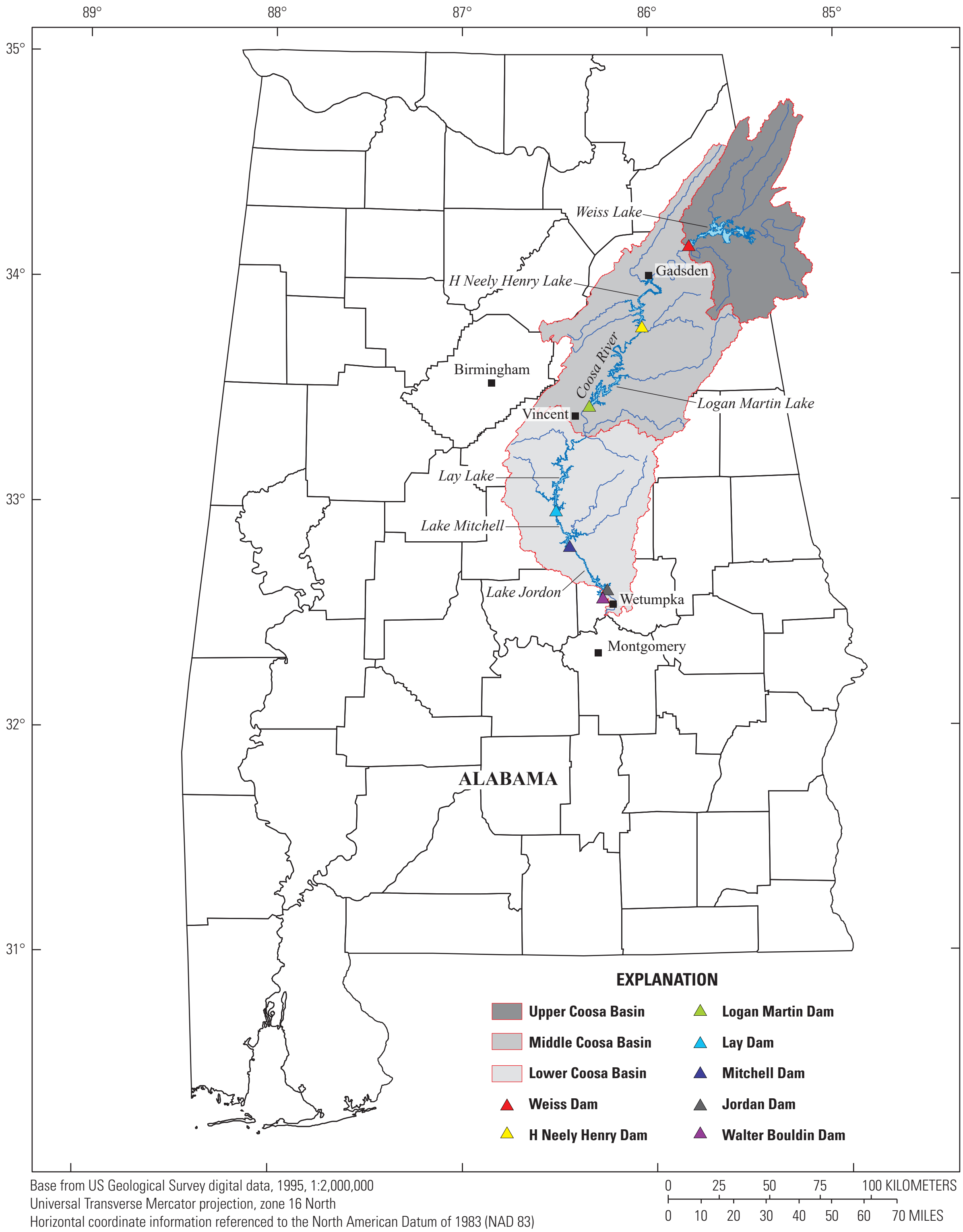

Figure 1. Location of the Coosa River Basin and associated dams in Alabama.

techniques may be dangerous and inadequate in supplying the necessary topographic detail for erosion-based analysis (Collins and others, 2007; Stock and others, 2011). T–lidar technology was used to document and quantify any changes in stream bank morphology during a 3-year period. Two surveys were conducted annually (generally in the summer and fall) for 3 years to determine channel geometry at specific bank locations above the water line. A comparison of the T–lidar datasets allow the U.S. Geological Survey and Alabama Power Company to quantify the approximate volume of bank material eroded from a given site.

Purpose and Scope

The purpose of this report is to document the results of periodic stream bank surveys completed from 2014 to 2017 at six locations downstream from three dams on the Coosa River in Alabama using T–lidar. Equipment and methods used and results obtained are described. The results obtained from the stream bank surveys document the conditions at the time of the surveys, and differences between surveys can be used to determine rates of erosion, which are correlated to streamflow conditions between surveys.

Description of Study Area

The study area included six survey sites on the Coosa River, consisting of two specific reach locations downstream from three selected dams: H Neely Henry Dam (fig. 2), Logan Martin Dam (fig. 3), and Walter Bouldin Dam (figs. 4–5). The location and length of these reaches was determined by the Alabama Power Company and stakeholders. The naming convention illustrated in figures 2–5 corresponds to Alabama Power Company's existing monitoring program. There are two survey sites downstream from H Neely Henry Dam: NH–104, a long reach on the right bank (fig. 2), and NH–108, a short reach on the left bank farther downstream (fig. 2). Downstream from Logan Martin Dam, site LM–102 on the right bank (fig. 3) was the subject of the previous study (Kimbrow and Lee, 2013); site LM–108 is the upstream end of an island near the right bank (fig. 3). Downstream from Walter Bouldin Dam, site WB–106 is on the right bank near the dam (fig. 4), whereas site WB–101 is on the left bank about 3.8 kilometers downstream from the dam (fig. 5).

Description of Flow Conditions

Hourly flows from H Neely Henry, Logan Martin, and Walter Bouldin Dams that represent flow through the generators and floodgates but do not include seepage flows were obtained from the Alabama Power Company (Keith E. Chandler, Alabama Power Company, written commun., 2018). Monthly mean flows were computed from the hourly flows for October 1, 2014, to September 30, 2017, and were generally lowest from May to November and highest from December to April, although flow conditions were highly variable during the study period (fig. 6). Alabama's proximity to the Gulf of Mexico results in increased precipitation during the late autumn, winter, and early spring when cold, dry continental air masses are forced southward by the polar jet stream and meet warm, moist maritime air originating over the gulf (Evans, 1999). Monthly flow conditions for H Neely Henry, Logan Martin, and Walter Bouldin Dams are described separately.

Hourly flow through H Neely Henry Dam generators and floodgates during October 1, 2014, to September 30, 2017, ranged from 0 cubic meters per second (m^3/s) on several days to 2,640 m^3/s at 4:00 a.m. on December 26, 2015. The median hourly flow during the period was 232 m^3/s. Monthly mean flow through H Neely Henry Dam ranged from 47.6 m^3/s during the month of November 2016 to 808 m^3/s during the month of December 2015 (fig. 6*A*). The median monthly flow during October 1, 2014, to September 30, 2017, was 169 m^3/s (fig. 6*A*).

Hourly flow through Logan Martin Dam generators and floodgates during October 1, 2014, to September 30, 2017, ranged from 0 m^3/s on several days to 2,120 m^3/s at 9:00 a.m. on December 28, 2015. The median hourly flow during the period was 171 m^3/s. Monthly mean flow through Logan Martin Dam ranged from 59.5 m^3/s during the month of November 2016 to 953 m^3/s during the month of January 2016 (fig. 6*B*). The median monthly flow during October 1, 2014, to September 30, 2017, was 193 m^3/s (fig. 6*B*).

Walter Bouldin Dam is on a diversion channel from Jordan Lake that flows into the Coosa River downstream from Jordan Dam. Because of this, flow characteristics of Walter Bouldin Dam differ from those of H Neely Henry and Logan Martin Dams. Flow from Jordan Lake is preferentially released through Jordan Dam for habitat maintenance on the Coosa River; therefore, it is not uncommon to have substantial periods of no flow from Walter Bouldin Dam. Hourly flow through Walter Bouldin Dam generators and floodgates during October 1, 2014, to September 30, 2017, ranged from 0 m^3/s on several days to 822 m^3/s at 12:00 p.m. on April 8, 2017. The median hourly flow during the period was 0 m^3/s. Monthly mean flow through Walter Bouldin Dam ranged from 1.70 m^3/s during the month of November 2016 to 656 m^3/s during the month of January 2016 (fig. 6*C*). The median monthly flow during October 1, 2014, to September 30, 2017, was 170 m^3/s (fig. 6*C*).

Data Collection Methods

Bank condition and stability at each site was determined using either a tripod- or boat-mounted T–lidar system. For all the surveys completed in this investigation, the primary instrument used was a Teledyne-Optech ILRIS High Density (HD) Enhanced Range (ER) laser scanner (Teledyne-Optech, 2012; figs. 7*A*, 7*B*); this is the same type of scanner that was used in

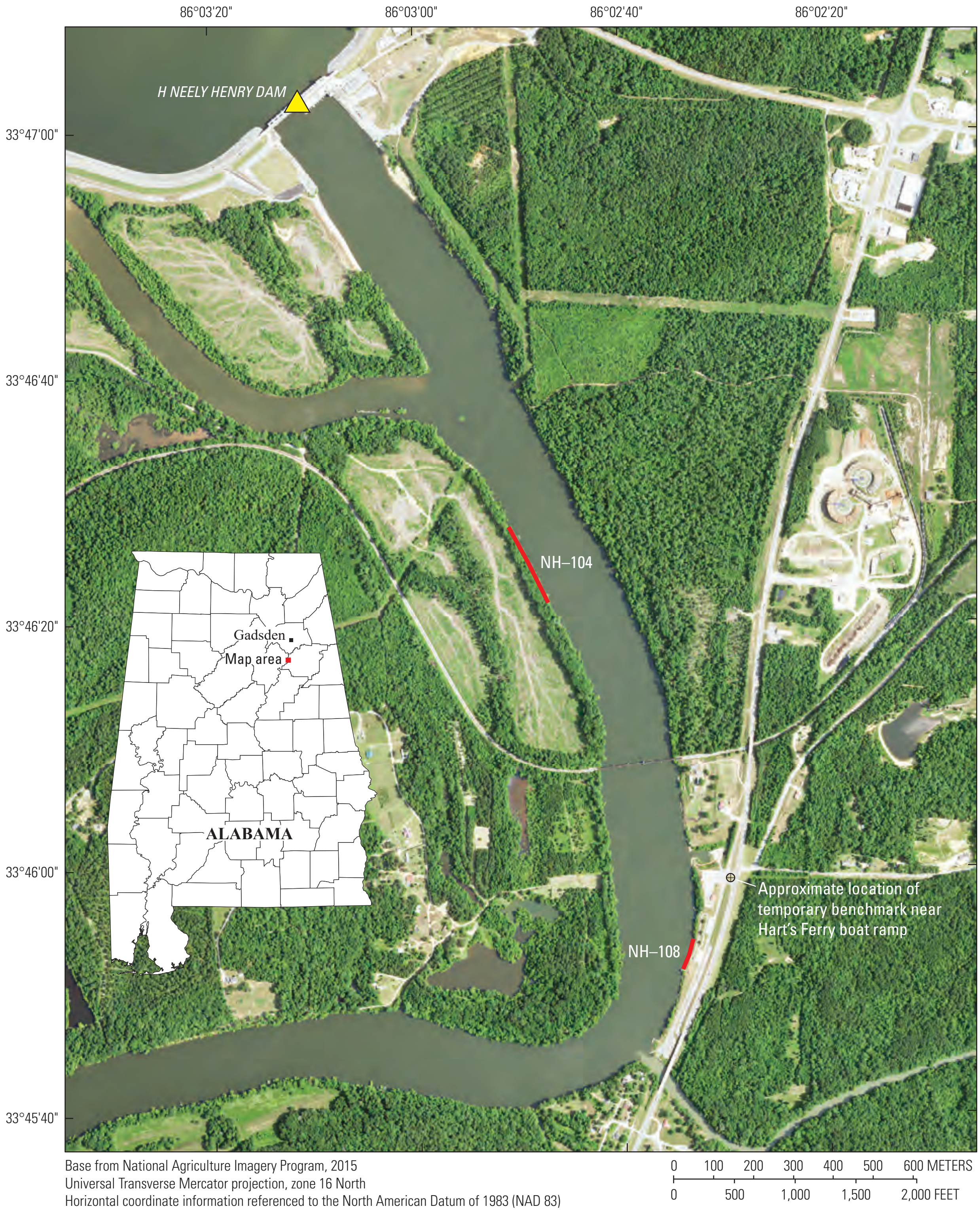

Figure 2. Location of survey sites NH–104 and NH–108 downstream from H Neely Henry Dam near Gadsden, Alabama.

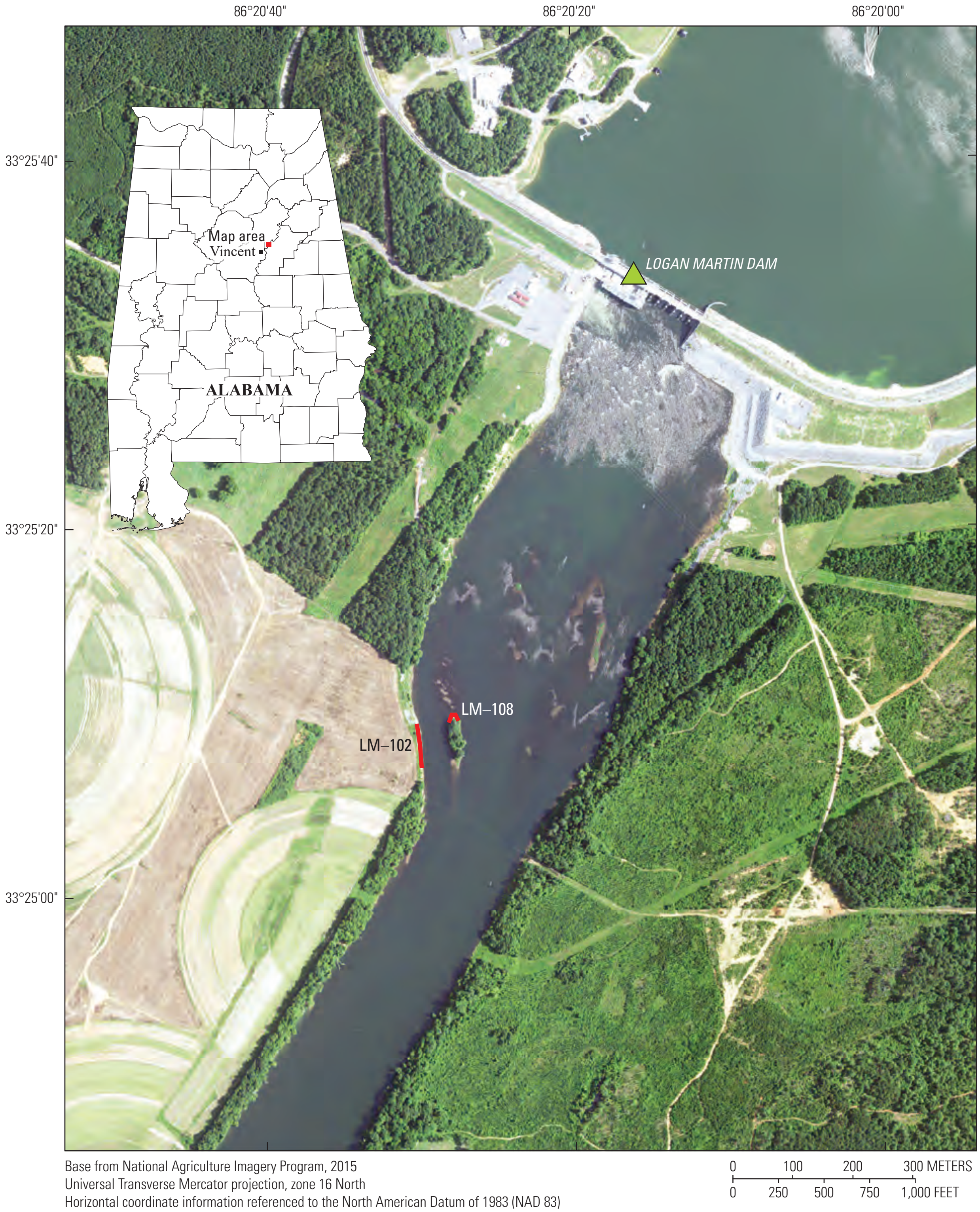

Figure 3. Location of survey sites LM–102 and LM–108 downstream from Logan Martin Dam near Vincent, Alabama.

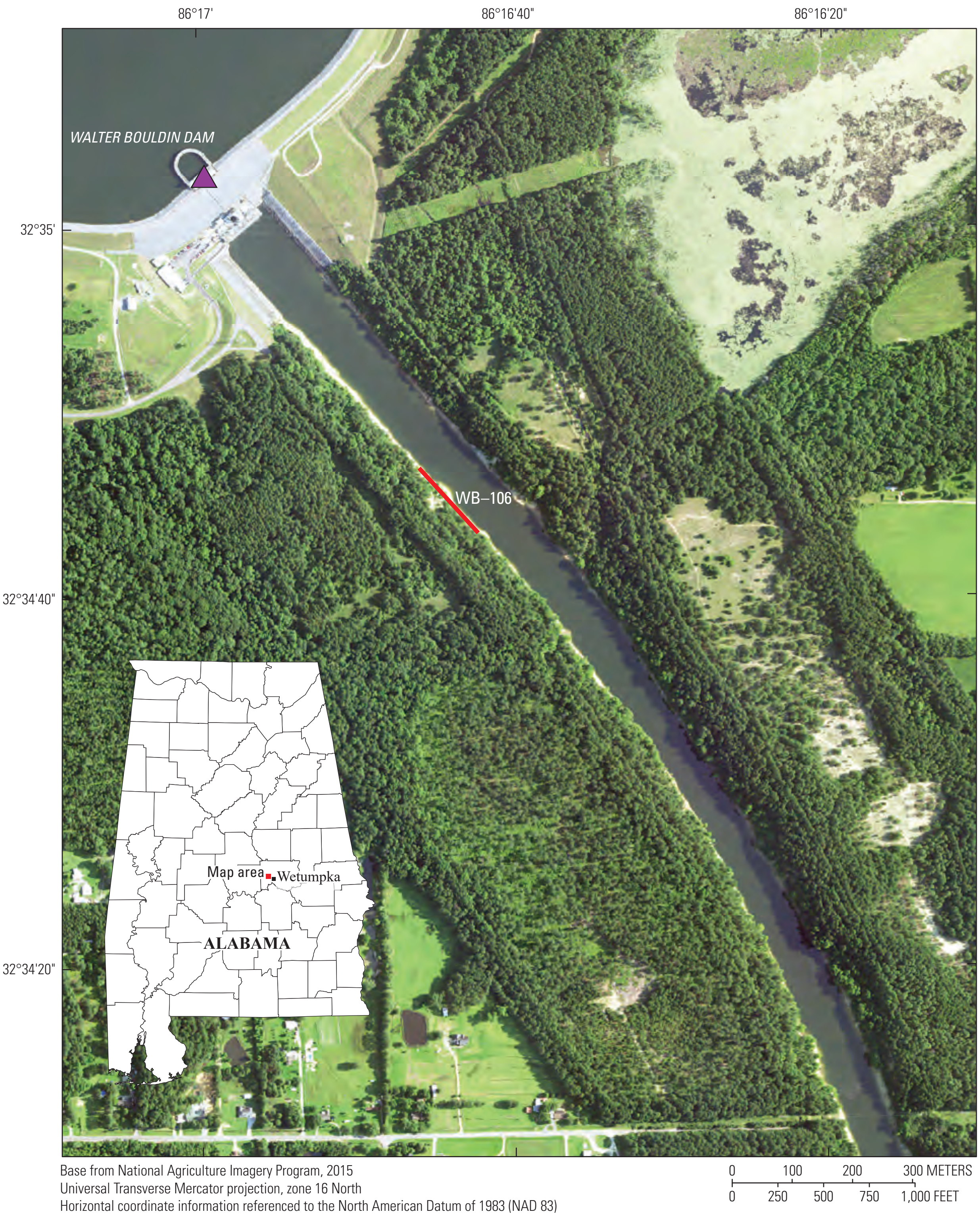

Figure 4. Location of survey site WB–106 immediately downstream from Walter Bouldin Dam near Wetumpka, Alabama.

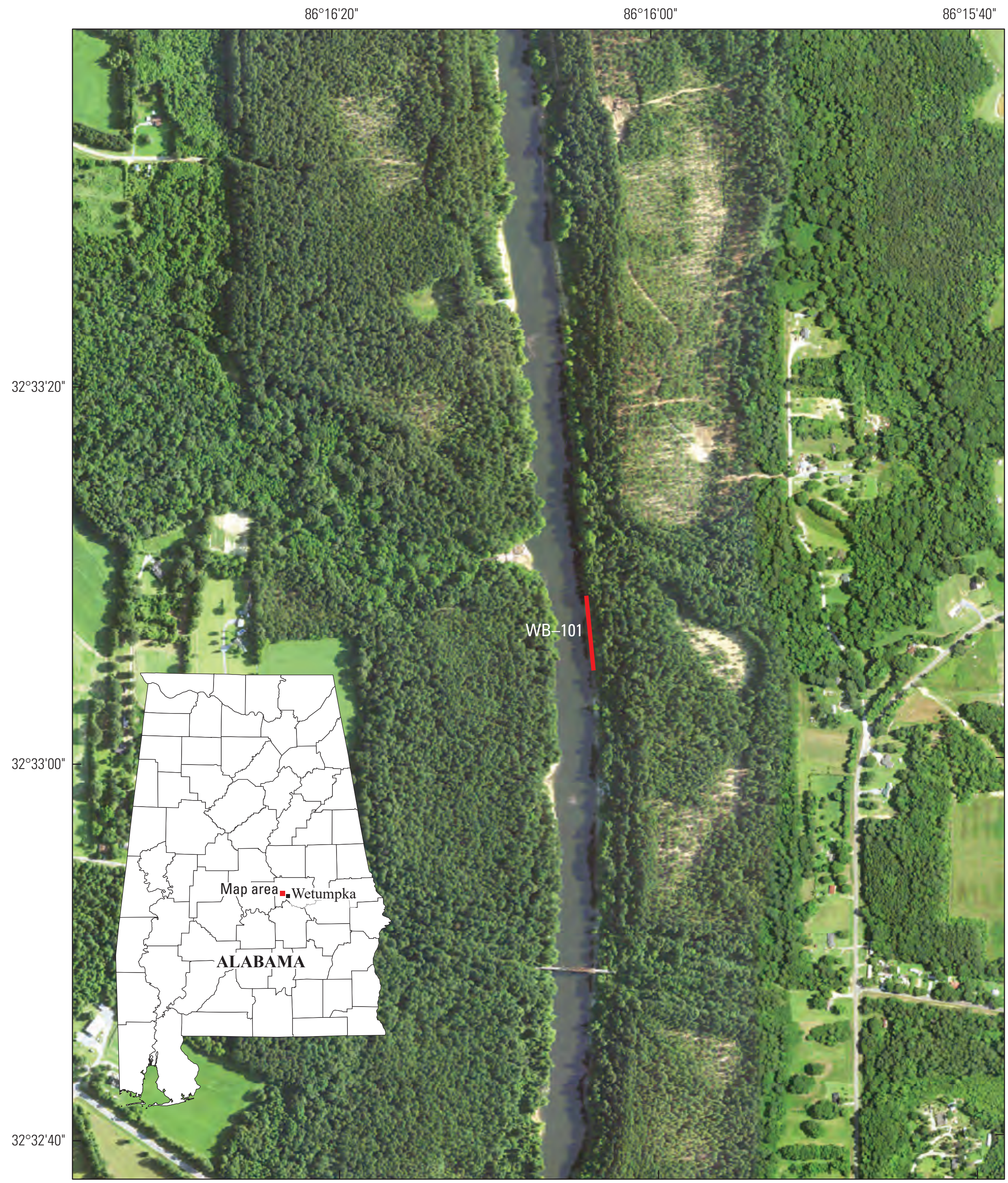

Figure 5. Location of survey site WB–101 3.8 kilometers downstream from Walter Bouldin Dam near Wetumpka, Alabama.

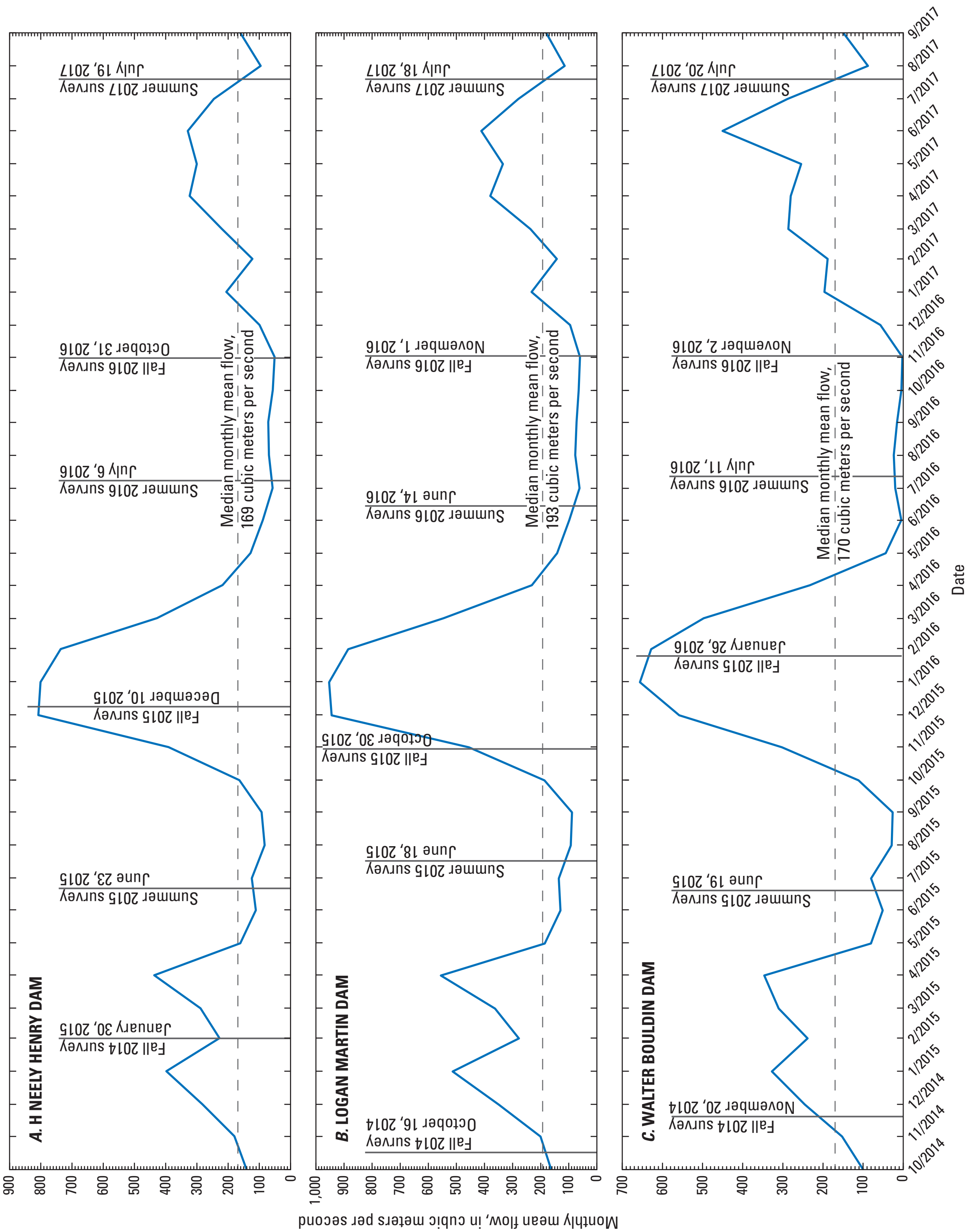

Figure 6. Monthly mean flows for H Neely Henry, Logan Martin, and Walter Bouldin Dams on the Coosa River in Alabama during October 2014 to September 2017.

Figure 7. The Teledyne-Optech ILRIS High Density Enhanced Range laser scanner mounted on *A*, a tripod with the pan/tilt base; *B*, a survey boat; and *C*, the FARO Focus^{3D} X 130 laser scanner used in this study.

a previous study at Logan Martin Dam, described in Kimbrow and Lee (2013). As described in the previous study (Kimbrow and Lee, 2013), T–lidar uses laser pulses that are sent from the instrument and reflected off objects within its field of view (FOV). It records the vertical and horizontal angle of each laser pulse relative to the instrument. The instrument calculates the distance of each returned laser pulse based on its round-trip time of travel and velocity. Although the primary T–lidar instrument is the same in both systems (boat- or tripod-mounted), the setup and data collection methods are somewhat different for each. The tripod-mounted T–lidar system was used to survey downstream from Logan Martin Dam, whereas the boat-mounted T–lidar system was used in surveys downstream from H Neely Henry and Walter Bouldin Dams.

Tripod-Mounted Terrestrial Light Detection and Ranging

The current study used a tripod-mounted system to survey the two sites downstream from Logan Martin Dam (LM–102 and LM–108; fig. 4). The ILRIS instrument was equipped with a pan/tilt base, allowing the scanner's standard 40 x 40 degree (°) FOV to be rotated 360° and also tilted vertically at any tripod setup point, if necessary. Topographic data were obtained by panning the T–lidar unit about 60° in discrete steps at a single tripod setup point on a gravel bar upstream from the surveyed reach to obtain enough data. Reference spheres were placed at known (relative) target points in the FOV of the lidar unit to assist in aligning each scan with prior scans. Data generally were collected from only one tripod setup point during each survey, and the region of interest (ROI) in the FOV was limited to the bank and island. The ROI would be broken into overlapping files any time the pan/tilt base was used to rotate the scanner to cover the total ROI.

In several of the surveys at Logan Martin, additional detail was collected for the island (site LM–108) using a FARO Focus^{3D} X 130 laser scanner. The FARO scanner is substantially smaller than the ILRIS HD ER (fig. 7*C*) with a more limited range; however, it can rapidly collect data in an about 130-meter (m) sphere around the unit. The smaller size and rapid data collection make the FARO scanner useful for "filling in" data gaps for limited survey areas. Topographical data were collected using the FARO scanner to supplement data gathered using the ILRIS HD ER. These supplemental data on the upstream face and top of the island were obtained by allowing the FARO unit to rotate 360° at two different tripod setups, one upstream from and one on top of the island. Reference spheres placed at various positions in the FOV of both T–lidar units were used to assist in aligning the scans from the same survey. The reference spheres on the bank target points (within the larger FOV and ROI of the ILRIS scanner) were used to align each scan with scans from previous surveys.

Boat-Mounted Terrestrial Light Detection and Ranging

The boat-mounted T–lidar system (hereinafter referred to as the "motion-compensated lidar" or "MC–lidar") was used in surveys at the sites downstream from H Neely Henry and Walter Bouldin Dams. The MC–lidar system consists of the T–lidar unit, an inertial navigation system (INS), and a data-collection and data-processing computer. The T–lidar unit is the same Teledyne-Optech ILRIS HD ER unit used for tripod-mounted surveys at Logan Martin Dam but is instead mounted to the roof of a boat without the pan/tilt base (fig. 7*B*). The INS that was used is the Applanix Position and Orientation Solution for Marine Vessels (POS-MV) WaveMaster system, which consists of two Global Navigation Satellite System (GNSS) receivers, an inertial motion unit (IMU), and a controller/processor. The INS provides position in three-dimensional space and measures the heave, pitch, roll, and heading of the vessel (and, thereby, the T–lidar unit) to accurately position the data received by the T–lidar unit. Position data from the INS were displayed in real time during the survey and logged for additional processing after the survey. A Topcon GR5 or Trimble model R8 GNSS base receiver was set on a local benchmark near each site to provide the post-processed kinematic (PPK) differential corrections to the INS for the navigation and tide solution after the survey. During surveys of sites downstream from H Neely Henry Dam, a temporary benchmark near the Hart's Ferry Boat Ramp (fig. 2) was occupied, for which high-accuracy National Spatial Reference System (NSRS) coordinates were determined using the National Geodetic Survey online positioning user service (OPUS; K.G. Lee, U.S. Geological Survey, written commun., 2016). During surveys of sites downstream from Walter Bouldin Dam, National Geodetic Survey benchmark PID CN3663, was occupied (see https://www.ngs.noaa.gov/cgi-bin/ds_mark.prl?PidBox=CN3363).

For an MC–lidar survey, the ROI is limited to a single vertical line in the FOV of the instrument, and data are essentially collected in a "fan" along that line as the boat moves (fig. 8). Topographic data were obtained along a longitudinal transect line along the bank of interest in multiple passes with different aspect angles and speeds to capture data from multiple directions in an effort to maximize the coverage.

Survey Data Processing

An initial processing step required for the MC–lidar data was to process the navigation information collected by the INS from the MC–lidar surveys using the POS-Pac Mobile Mapping Suite (MMS) software (Applanix Corporation, 2009). POS-Pac MMS provides tools to identify and compensate for sensor and environmental errors and computes an optimally blended navigation solution from the GNSS and IMU raw data. The blended navigation solution (called a "smoothed best estimate of trajectory" or "SBET" file) generated by

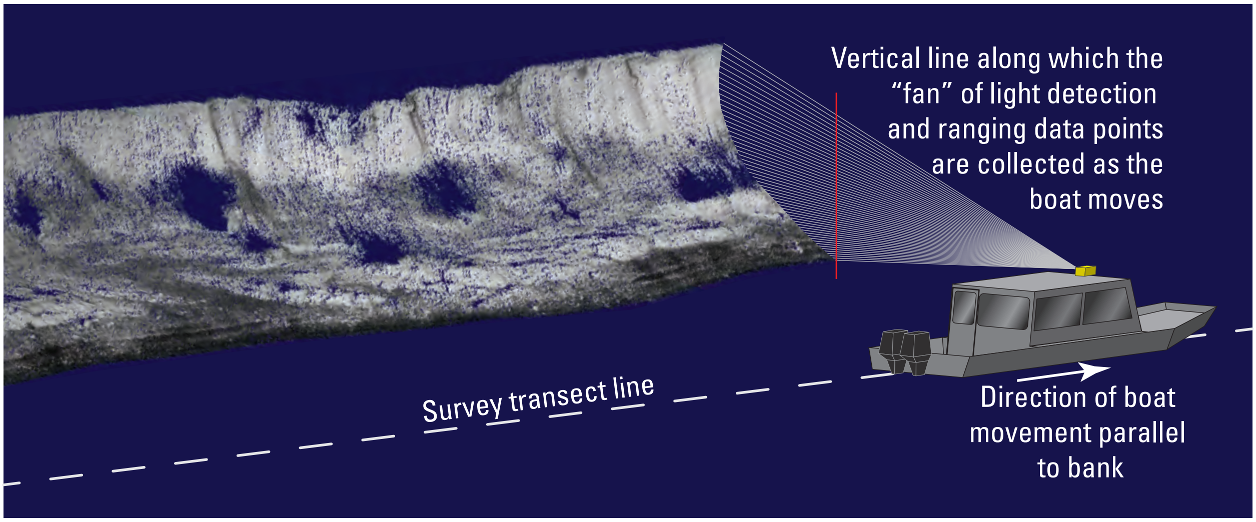

Figure 8. Conceptual rendition of stream bank data collection using the boat-mounted light detection and ranging system.

postprocessing the navigation data was applied to the survey at a given site to properly position the accumulated lidar data in three-dimensional space.

The data from the T–lidar and INS components (when used) were parsed, processed, and integrated into cohesive datasets for visualization and cleanup. The ILRIS T–lidar data from the tripod-mounted surveys were parsed in the Teledyne-Optech Parser executable (Teledyne-Optech, 2012) to process the raw data into multiple XYZ datasets with signal return intensity, one for each pivot step at the tripod setup. For MC–lidar surveys, the parsing step included combining the raw T–lidar data with the necessary offset and orientation parameters contained in a boresight calibration file (explained in the "Survey Data Quality Assurance and Accuracy" section below) and georeferencing the data using the navigation and position solution data from the SBET file from POS-Pac MMS. The MC–lidar data were output to multiple XYZ datasets with intensity, one for each survey transect line pass. The FARO data (when used) were processed in the FARO Scene software (FARO Technologies, Inc., 2016), which allows multiple FARO scan files to be aligned using the reference targets and common topographic features between the scan files and output to multiple XYZ datasets with intensity, one for each scanner setup location.

The various XYZ files for a given survey were combined into a single topographic dataset and visualized in the PolyWorks IM-Align and IM-Survey software packages, which create a surface model of the data for a given survey (Innovmetric, 2012). The data were referenced and aligned with prior surveys using coordinates for the various target reference spheres in the surveyed area. These target reference spheres also were used to improve the alignment of the various MC–lidar surveys with prior surveys; although the MC–lidar surveys are georeferenced in three-dimensional space through the SBET file, minor differences in the location of these target spheres were observed between surveys, which are the result of subtle variations in vessel setup, atmospheric conditions during the survey, and error associated with using a motion-compensation system.

After alignment, the T–lidar point clouds were further processed to remove as much vegetation as possible. The final dataset for each survey location and date consisted of essentially bare earth topography. The processed and cleaned data were output to a space-delimited file XYZ dataset with intensity, one for each survey at each site, and are available as a U.S. Geological Survey data release (Huizinga and Wagner, 2019).

The various final T–lidar XYZ point clouds for a given site were compared to one another using the Multiscale Model-to-Model Cloud Comparison (M3C2) plugin in the CloudCompare software (CloudCompare, 2018; Lague and others, 2013). The M3C2 plugin computes signed and robust distances directly between two point clouds at core points subsampled from the first cloud. The M3C2 distance was computed along a horizontal axis that would provide the most meaningful result (into the face of the bank). A variety of parameters can be chosen by the user, such as a subsample distance for core points, which is the distance at which the full-density point cloud is subsampled to improve speed of computation in the comparison; a normal scale, which is the diameter of the spherical neighborhood extracted around each core point to compute a local normal and used to orient a cylinder inside which equivalent points are searched for in the second cloud; a projection scale, which is the diameter of the cylinder used to search for equivalent points in the second point cloud; and a maximum depth, which is the height of the cylinder used to search for equivalent points in the second point cloud. The values for these parameters were determined empirically for each survey site to optimize the view of the comparison cloud while minimizing computation time. A point cloud representing the output of the M3C2 plugin was saved as an XYZ file in American Standard Code for Information

Interchange (referred to as “ASCII”) format, with additional attributes generated by the tool. These data files also are included with metadata in Huizinga and Wagner (2019).

Volume gain or loss between scans was computed using the 2.5D Volume tool in the CloudCompare software (CloudCompare, 2018). The tool creates a gridded (raster) surface of each point cloud and computes the difference in volume along a user-selected axis, generally chosen to provide the most meaningful result (into the face of the bank), using a cell size that was similar to the core point subsample distance used in the M3C2 plugin. Each cell was assigned the average value of points within the cell, and the values of empty cells generally were interpolated from surrounding cells. However, two survey areas (Walter Bouldin sites WB–101 and WB–106) had a substantial percentage of empty cells due to dense vegetation obscuring the bank during the surveys. Interpolation of empty cells in these areas resulted in unrealistic volume computations; therefore, the empty cells were left empty for these two sites.

Survey Data Quality Assurance and Accuracy

Survey methods used to obtain tripod-mounted T–lidar data were similar to those described in Kimbrow and Lee (2013). A surveying methodology was used with the intent of one-sided coverage of features in the ROI. These data were supplemented with additional scans from the smaller FARO scanner to fill in small missing areas when feasible.

For the MC–lidar system, the principal quality-assurance measures were a boresight calibration test used to determine the positional and angular offsets of the MC–lidar unit and assessment of the INS in real time during the survey to ensure quality of the acquired data. Data acquired by the MC–lidar system were nominally viewable in real time during the latter two surveys, but a surveying methodology was used in all the MC–lidar surveys with the intent of one-sided coverage (from the water) of features in the ROI. Multiple passes using different aspect angles were made along the surveyed reach to reduce any “shadows” behind smaller objects resulting from a single pass.

Boresight Calibration Test

A boresight calibration test is used to check for subtle variations in the orientation of the T–lidar unit with respect to the INS and real-world coordinates (Teledyne-Optech, 2012). In a boresight calibration test, the angular offsets to roll, pitch, and yaw caused by the alignment of the T–lidar unit and the INS on the survey vessel were determined for each scan direction (port or starboard) of the T–lidar unit on each boat.

For a boresight calibration test, all instrumentation (T–lidar, IMU, and GNSS antennae) must first be surveyed, and their relative positions (lever arms) must be resolved with respect to the origin point of the IMU. Determination of the angular offsets involves surveying at least three targets with traditional methods in real-world, earth-centered, earth-fixed coordinates and then scanning those same targets using the MC–lidar system (which has been mounted on the boat) while the boat is held stationary but collecting INS data. The Teledyne-Optech MatchView executable (Teledyne-Optech, 2012) is then used to derive the angular differences necessary to align the T–lidar points to their real-world coordinates. The output boresight calibration file contains the identified and quantified lever arms and angular offsets.

The offsets obtained from a boresight test are assumed to be essentially constant for a given boat and directional configuration (Teledyne-Optech, 2012), provided the T–lidar is mounted in the same location and configuration each time. Alignment brackets were used on both survey boats in this study to ensure consistent re-location of the T–lidar each time it was used for the MC–lidar system. The lever arm and angular offsets determined in the boresight calibration test are applied when processing the data collected from a given MC–lidar survey.

Error Estimation

The errors associated with the collection of topographic data can be classified as systematic or random. Systematic errors are those that can be measured or modeled through calibration (Byrnes and others, 2002). Random errors are a result of the limitations of the measuring device and an inability to perfectly model the systematic errors. Therefore, the overall accuracy of a point cloud dataset collected using T–lidar is limited by three factors: laser error, alignment error, and georeferencing error (Collins and others, 2009). Laser error is inherent to all data acquired by the laser scanner and is 0.008 m for the Teledyne-Optech ILRIS HD ER scanner as stated by the manufacturer (Teledyne-Optech, 2012) and 0.002 m for the FARO Focus^{3D} X 130 scanner as stated by the manufacturer (FARO Technologies, Inc., 2014).

Alignment and georeferencing errors are generally synonymous in the MC–lidar surveys. The errors reported for the MC–lidar surveys (table 1) are related to the positional accuracy of the INS when collecting the topographic data and are based on the minimum and maximum observed peak-to-peak root mean square errors. As discussed in the “Survey Data Processing” section above, although the MC–lidar data are georeferenced in three-dimensional space through the SBET file, minor differences in the location of these target spheres were observed between surveys, which likely are the result of subtle variations in vessel setup, atmospheric conditions during the survey, and error associated with using a motion-compensation system (table 1). These differences in alignment were minimized using the target reference spheres in the MC–lidar surveys.

The horizontal and vertical alignment errors for each of the tripod-mounted T–lidar surveys at Logan Martin Dam (relative to the reference scan on June 18, 2015) were determined based on the difference between the easting, northing, and elevation values of virtual reference points at the centers

Table 1. Minimum and maximum horizontal and vertical errors from boat-mounted terrestrial light detection and ranging surveys at selected bank locations downstream from H Neely Henry and Walter Bouldin Dams on the Coosa River in Alabama, 2014–17.

[RMSE, root mean square error; m, meter]

Survey date	Horizontal RMSE		Vertical RMSE	
	Mimimum (m)	Maximum (m)	Mimimum (m)	Maximum (m)
H Neely Henry Dam				
1/30/2015	0.004	0.013	0.008	0.038
6/23/2015	0.010	0.022	0.038	0.047
12/10/2015	0.005	0.011	0.007	0.014
7/6/2016	0.004	0.009	0.006	0.013
10/31/2016	0.019	0.025	0.049	0.055
7/19/2017	0.014	0.019	0.039	0.046
Walter Bouldin Dam				
11/20/2014	0.005	0.014	0.008	0.029
6/19/2015	0.006	0.024	0.008	0.021
1/26/2016	0.012	0.018	0.028	0.030
7/11/2016	0.018	0.034	0.063	0.070
11/2/2016	0.016	0.021	0.032	0.038
7/20/2017	0.011	0.020	0.034	0.042

Table 2. Horizontal and vertical alignment errors relative to the reference scan on June 18, 2015, from tripod-mounted terrestrial light detection and ranging surveys at selected bank locations downstream from Logan Martin Dam on the Coosa River in Alabama, 2014–17.

[m, meter]

Survey date	Horizontal error (m)	Vertical error (m)
10/16/2014	0.0050	0.0001
6/18/2015	[a]0	[a]0
10/30/2015	0.0055	0.0031
6/14/2016	0.0058	0.0021
11/1/2016	0.0069	0.0001
7/18/2017	0.0041	0.0000

[a]The survey of June 18, 2015, was used as the “reference” survey to which all other surveys were aligned. This survey was used to approximately georeference all the Logan Martin surveys using Global Navigation Satellite System (GNSS) coordinates for two of the three reference spheres and the surveyed water-surface elevation as a verification. The overall horizontal error of the georeferencing (the difference between the GNSS coordinates and the virtual coordinates of the targets) was 0.011 meter, and the overall vertical error was 0.040 meter.

of the reference spheres on the bank of site LM–102 and the easting, northing, and elevation values of the sphere center points in the June 18, 2015 survey (table 2). The real-world coordinates for the sphere center points were determined using GNSS on June 18, 2015, at the site; hence, there is no alignment error for that survey.

All the Logan Martin Dam surveys were then approximately georeferenced to real-world coordinates using GNSS coordinates obtained for two of the reference spheres on the bank at site LM–102 for the reference scan on June 18, 2015. A minimum of three targets are necessary for full georeferencing to fully account for three-dimensional position and orientation. However, approximate position and orientation of the points could be obtained using the two targets, and additional orientation verification was afforded by the water-surface elevation, which was assumed to be level between the island and bank for the reference scan. The error between the GNSS coordinates and the virtual reference points at the center of the two reference spheres was determined to be 0.011 m in the horizontal and 0.040 m in the vertical, and can be considered the overall georeferencing error for the Logan Martin surveys. However, the small horizontal and vertical alignment errors relative to the reference scan on June 18, 2015, indicate that the surveys are closely aligned with each other and the magnitude of the alignment errors is small compared to the georeferencing error (table 2).

Erosion Monitoring using Terrestrial Light Detection and Ranging Surveys

The site-specific results for each dam site are discussed in the following sections, from upstream to downstream. All elevation data were referenced to the North American Vertical Datum of 1988 (NAVD 88).

In the following sections, erosion (or deposition) values are reported in terms of a “normalized” value. The normalized erosion (or deposition) is computed as the total net erosion (or deposition) between the scan surfaces for a given time interval, divided by the surface area common to both surfaces, and reported in cubic meters per square meter. This normalized value is intended to aid in the comparability of the values for the vastly different areal extents of the sites.

H Neely Henry Dam, Sites NH–104 and NH–108

Daily mean flow through H Neely Henry Dam generators and floodgates (not including seepage) during October 1, 2014, through September 30, 2017, was computed from hourly flows provided by the Alabama Power Company. Daily mean flow ranged from 0 to 2,140 m^3/s, and the median daily mean flow was 140 m^3/s (fig. 9).

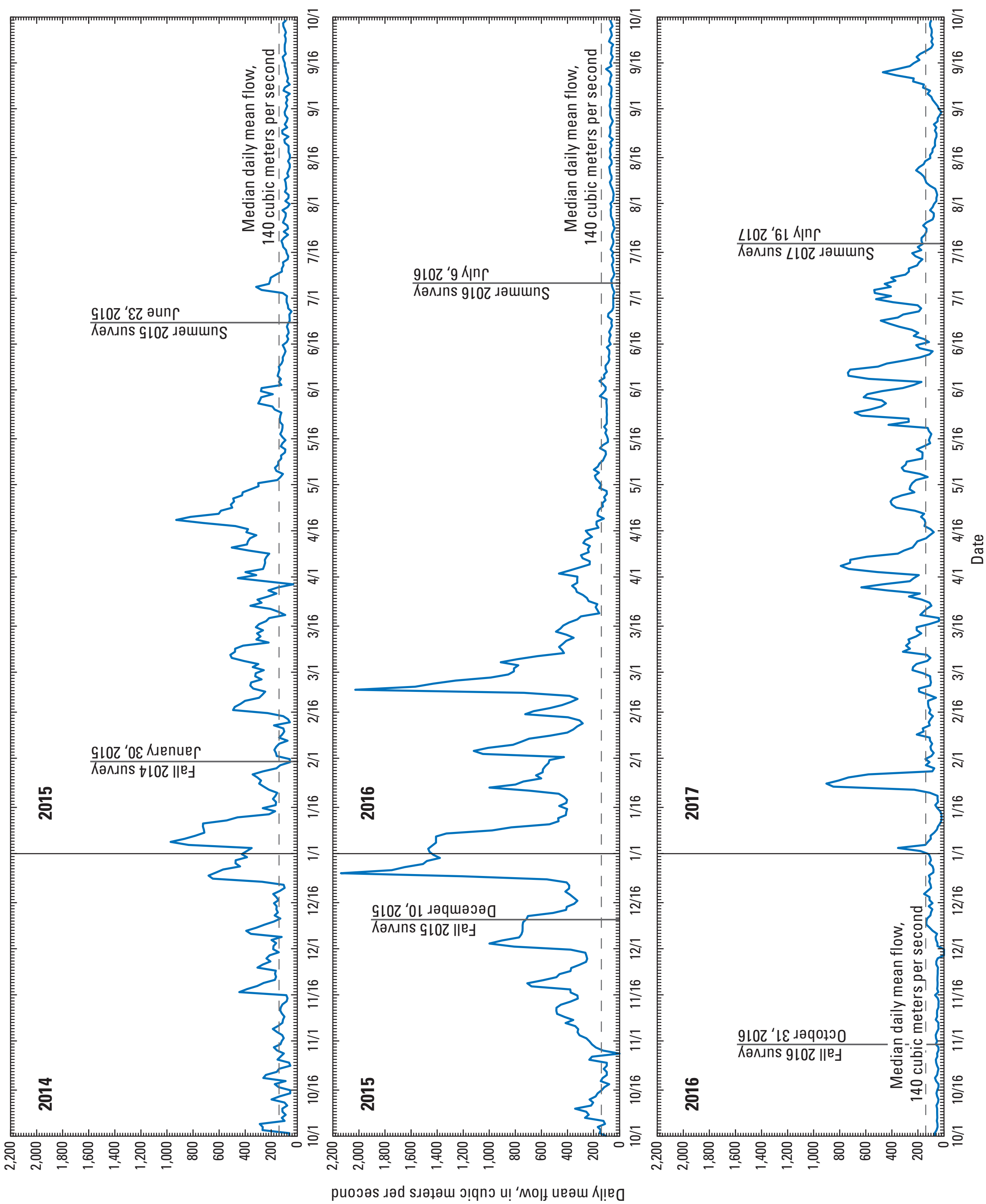

Figure 9. Daily mean flow on the Coosa River downstream from H Neely Henry Dam near Gadsden, Alabama, for October 1, 2014, to September 30, 2017, by water year, with survey dates indicated.

Site NH–104

Comparison of the fall 2014 (January 2015) and summer 2017 (July 2017) T–lidar scans (fig. 10) of site NH–104 indicated a normalized erosion of 0.273 cubic meters per square meter (m^3/m^2) (table 3). The largest differences between the scans occurred at bank failures apparent near the upstream and downstream ends of the bank, where greater than 0.5 m of erosion was indicated (fig. 10*G*).

Net erosion was observed during four of the five intervals between T–lidar scans, with the greatest amount, 0.154 m^3/m^2, occurring between the summer 2015 and fall 2015 (June and December 2015) scans (table 3). About 0.5 m of erosion was indicated near the upstream end of the bank at the location of a bank failure and corresponding deposit at the toe of the bank (fig. 10*C*). Although daily mean flows through H Neely Henry Dam during the June to December 2015 interval were not of the highest magnitude experienced during the study, above-median and generally increasing daily mean flow occurred from October 1, 2015, until the day of the scan on December 10, 2015 (fig. 9). The maximum daily mean flow during the summer to fall 2015 interval, 1,000 m^3/s, occurred on December 3, 2015, just 1 week before the scan on December 10, and daily mean flows exceeded 730 m^3/s from December 2 to 10 (fig. 9).

Net deposition of 0.013 m^3/m^2 occurred between the summer 2016 (July 2016) and fall 2016 (October 2016) scans (table 3). Relatively minor, somewhat uniform deposition of less than 0.2 m between surveys was observed along the bank (fig. 10*E*). Daily mean flows during the July to October 2016 period were below the median of 140 m^3/s (fig. 9).

Site NH–108

Comparison of the fall 2014 (January 2015) and summer 2017 (July 2017) T–lidar scans of site NH–108 indicated net erosion of 0.165 m^3/m^2 during the study (table 3). The largest differences between the scans occurred at bank failures apparent near the upstream end of and near the center of the top of the bank, where greater than 0.5 m of change was indicated (fig. 11*G*).

Net erosion was observed during three of the five intervals between T–lidar scans, with the greatest amount of normalized erosion, 0.098 m^3/m^2, occurring between the fall 2015 (December 2016) and summer 2016 (July 2016) scans (table 3). Greater than 0.5 m of change was indicated at two areas of bank failure, one near the top of the upstream end of the bank (with a corresponding deposit at the toe of the bank) and the other near the center of the top of the bank (fig. 11*D*). Daily mean flows through H Neely Henry Dam during the fall 2015 to summer 2016 interval included those of the greatest magnitude experienced during the study. A long duration of above-median flow occurred from the fall 2015 scan on December 10 through the end of April 2016, followed by a period of near- to below-median flow from May 1, 2016, through the date of the summer 2016 scan on July 6 (fig. 9).

Net deposition was observed during two of five intervals, summer 2015 to fall 2015 and summer 2016 to fall 2016. Similar amounts of normalized deposition, 0.029 and 0.031 m^3/m^2, respectively, were observed during the two intervals, and relatively minor, uniform change of less than about 0.2 m was observed along the bank (table 3; fig. 11*E*). Daily mean flows during the summer to fall 2015 period were generally below the median of 140 m^3/s from the date of the summer 2015 scan on June 23 through October and were above-median from November through the date of the fall 2015 scan on December 10. Daily mean flows during the summer to fall 2016 period were below the median of 140 m^3/s (fig. 9).

Logan Martin Dam, Sites LM–102 and LM–108

Daily mean flow through Logan Martin Dam generators and floodgates (not including seepage) during October 1, 2014, through September 30, 2017, was computed from hourly flows provided by the Alabama Power Company. Daily mean flow ranged from 24.1 to 2,120 m^3/s, and the median was 158 m^3/s (fig. 12).

Flow through the Logan Martin Dam generators and floodgates was halted the evening before each of the scans at the Logan Martin sites to ensure the low-lying island was not inundated. Therefore, only flow from seepage through the dam occurred during each scan, which resulted in relatively similar water-surface elevations in all of the scans.

Site LM–102

Comparison of the fall 2014 (October 2014) and summer 2017 (July 2017) T–lidar scans (fig. 13) of site LM–102 indicated normalized erosion of 0.419 m^3/m^2 during the study (table 3). The difference between the scans exceeded 0.5 m along much of the vertical part of the bank (fig. 13*G*).

Net erosion was observed during all five intervals between T–lidar scans, with the greatest amount of normalized erosion, 0.161 m^3/m^2, occurring between the fall 2015 (October 2015) and summer 2016 (June 2016) scans (table 3). A large area of greater than 0.5 m of change was indicated near the upstream end of the bank (fig. 13*D*). During nearly all of the interval between the fall 2015 and summer 2016 scans, daily mean flows through Logan Martin Dam exceeded the median of 158 m^3/s, and the two greatest magnitude daily mean flows experienced during the study, 2,120 m^3/s on December 28, 2015, and 1,740 m^3/s on February 26, 2016, also occurred during the period (fig. 12).

The least amount of normalized erosion between T–lidar scans, 0.019 m^3/m^2, occurred between the summer 2015 (June 2015) and fall 2015 (October 2015) scans (table 3). Relatively minor, uniform change of less than 0.1 m was observed along the bank (fig. 13*C*). Daily mean flows during the summer to fall 2015 interval were below the median of 158 m^3/s most of the time (fig. 12).

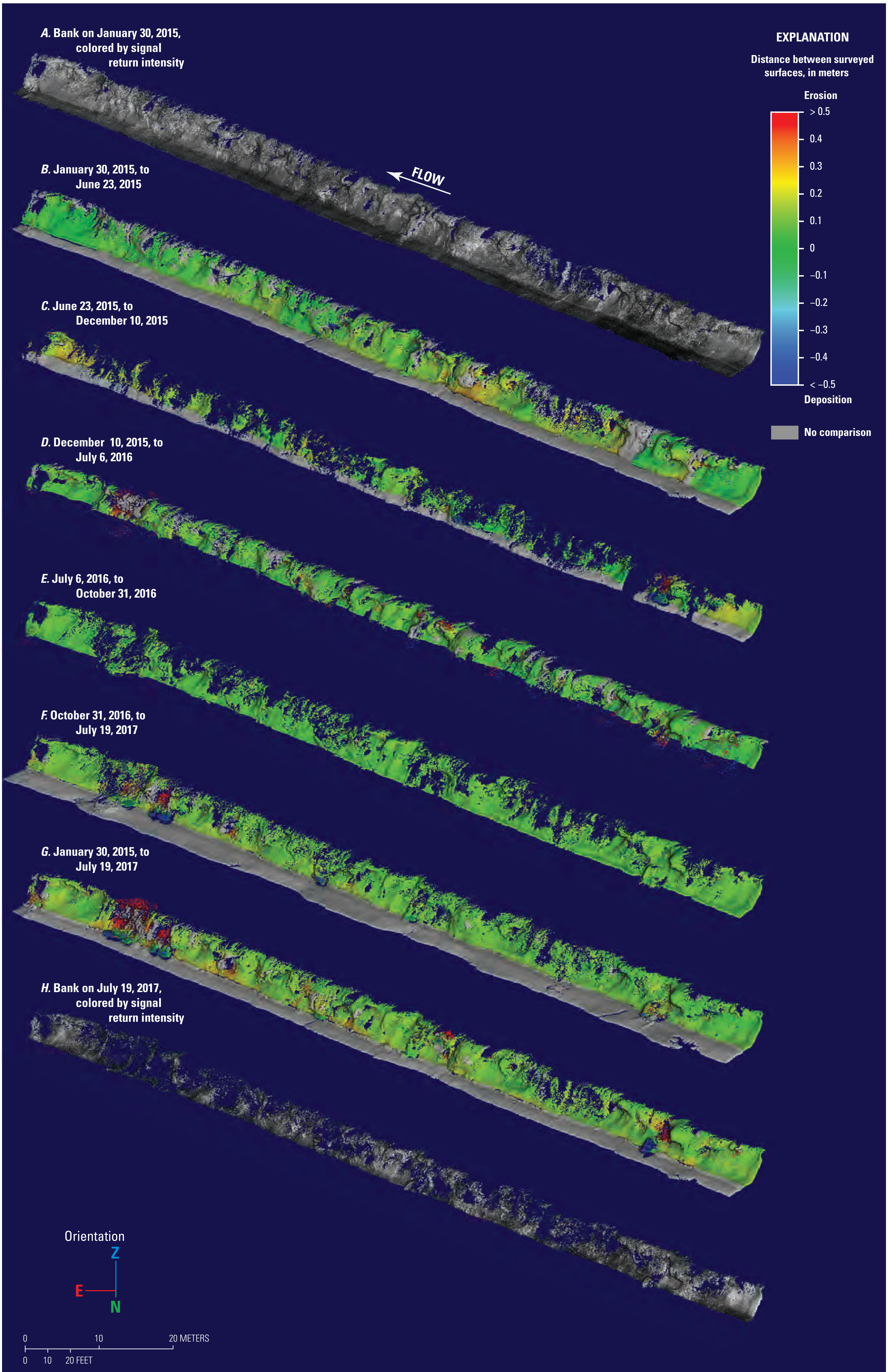

Figure 10. Surveyed banks and incremental differences between surveys at H Neely Henry Dam site NH–104 on the Coosa River near Gadsden, Alabama, for January 30, 2015, through July 19, 2017. *A*, bank on January 30, 2015, colored by signal return intensity; *B*, January 30, 2015, to June 23, 2015; *C*, June 23, 2015, to December 10, 2015; *D*, December 10, 2015, to July 6, 2016; *E*, July 6, 2016, to October 31, 2016; *F*, October 31, 2016, to July 19, 2017; *G*, January 30, 2015, to July 19, 2017; and *H*, bank on July 19, 2017, colored by signal return intensity.

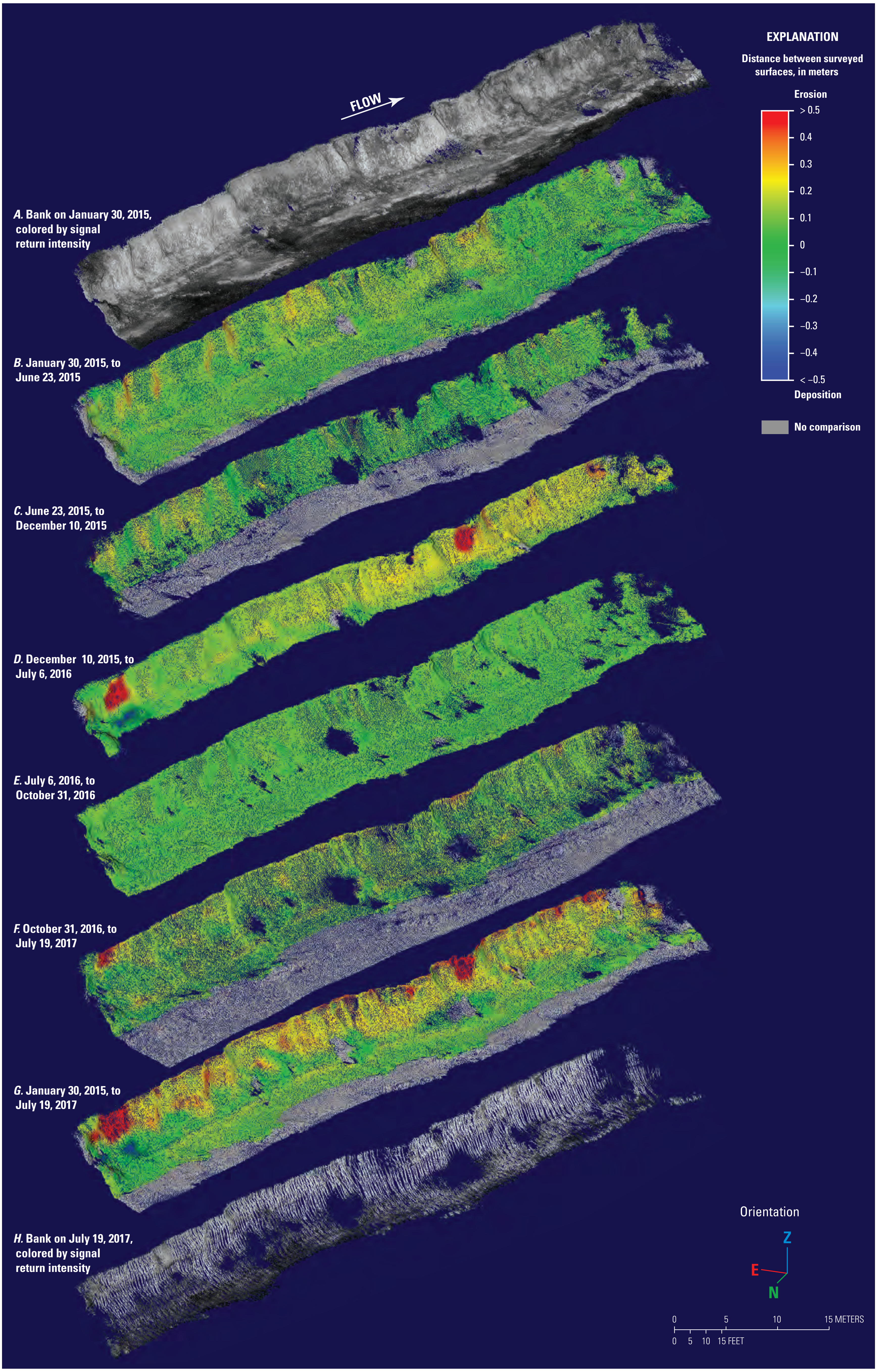

Figure 11. Surveyed banks and incremental differences between surveys at H Neely Henry Dam site NH–108 on the Coosa River near Gadsden, Alabama, for January 30, 2015, through July 19, 2017. *A*, bank on January 30, 2015, colored by signal return intensity; *B*, January 30, 2015, to June 23, 2015; *C*, June 23, 2015, to December 10, 2015; D, December 10, 2015, to July 6, 2016; *E*, July 6, 2016, to October 31, 2016; *F*, October 31, 2016, to July 19, 2017; *G*, January 30, 2015, to July 19, 2017; and *H*, bank on July 19, 2017, colored by signal return intensity.

Table 3. Total net and normalized erosion for selected intervals at selected bank locations of the Coosa River in Alabama from terrestrial light detection and ranging technology.

[Negative values indicate deposition]

Survey site	Selected interval					
	Fall 2014 to summer 2015	Summer 2015 to fall 2015[a]	Fall 2015 to summer 2016[a]	Summer 2016 to fall 2016	Fall 2016 to summer 2017	Fall 2014 to summer 2017
Total net erosion volume, in cubic meters						
NH–104	8.85	113	54.3	−13.6	101	256
NH–108	13.6	−9.33	32.7	−13.8	38.0	65.4
LM–102	34.4	7.36	50.7	6.95	42.4	159
LM–108[b]	1.14	7.27	12.7	−1.66	10.2	23.1
WB–101	27.7	−7.01	74.6	−146	76.1	77.4
WB–106	232	−268	−127	1,170	235	1,310
Normalized erosion[c], in cubic meters per square meter						
NH–104	0.009	0.154	0.074	−0.013	0.106	0.273
NH–108	0.032	−0.029	0.098	−0.031	0.086	0.165
LM–102	0.090	0.019	0.161	0.022	0.109	0.419
LM–108[b]	0.099	0.573	0.692	−0.100	0.572	2.05
WB–101	0.068	−0.025	0.226	−0.196	0.199	0.331
WB–106	0.084	−0.121	−0.066	0.457	0.083	0.467

[a]The “summer 2015 to fall 2015” and “fall 2015 to summer 2016” intervals likely are biased by the relatively smaller bank area that could be surveyed during the fall 2015 survey.

[b]Site LM–108 is an island, and the surveyed area is the part that experiences head-on flow, as compared with the shear flow experienced by all the other sites.

[c]The normalized erosion is computed as the total net erosion for the interval divided by the surface area common to both survey areas.

Site LM–108

Comparison of the fall 2014 (October 2014) and summer 2017 (July 2017) T–lidar scans of site LM–108, an island in the Coosa River, indicated normalized erosion of 2.05 m^3/m^2 during the study (table 3).This is the largest amount of normalized erosion of all the surveyed sites, likely because the surveyed area experiences head-on flow from the river, compared with the other sites experiencing predominantly shear flow. The difference between the scans exceeded 1.0 m on much of the upstream end and right (west) side of the island (fig. 14*G*). Bank retreat at the upstream end of the island (using a narrow band of data near the water line common in all the scans) during the study is estimated to be 2.9 m (fig. 15).

Net erosion was observed during four of the five intervals between T–lidar scans, with the greatest amount of normalized erosion, 0.692 m^3/m^2, occurring between the fall 2015 (October 2015) and summer 2016 (June 2016) scans (table 3). Greater than 0.5 m of change was indicated near the upstream end of the island and along the right (west) side of the island (fig. 14*D*). During the interval between the fall 2015 and summer 2016 scans, nearly all daily mean flows exceeded the median of 158 m^3/s, and the two greatest magnitude daily mean flows through Logan Martin Dam that were experienced during the study, 2,120 m^3/s on December 28, 2015, and 1,740 m^3/s on February 26, 2016, also occurred during the period (fig. 12).

Normalized deposition of 0.100 m^3/m^2 occurred between the summer 2016 (June 2016) and fall 2016 (November 2016) scans (table 3). Relatively minor and uniform change of less than about 0.2 m was observed on the surveyed part of the island, although a few areas at the upstream end and along the right (west) side of the island experienced about 0.5 m of erosion (fig. 14*E*). Daily mean flows during the summer to fall 2016 interval were below the median of 158 m^3/s (fig. 12).

Walter Bouldin Dam, Sites WB–101 and WB–106

Daily mean flow through Walter Bouldin Dam generators and floodgates (not including seepage) during October 1, 2014, through September 30, 2017, was computed from hourly flows provided by the Alabama Power Company. Daily mean flow ranged from 0 to 809 m^3/s, and the median was 114 m^3/s (fig. 16). As explained in the “Description of Flow Conditions” section above, flow from Jordan Lake is preferentially released through Jordan Dam for habitat maintenance on the Coosa River; therefore, it is not uncommon to have substantial periods of no flow from Walter Bouldin Dam.

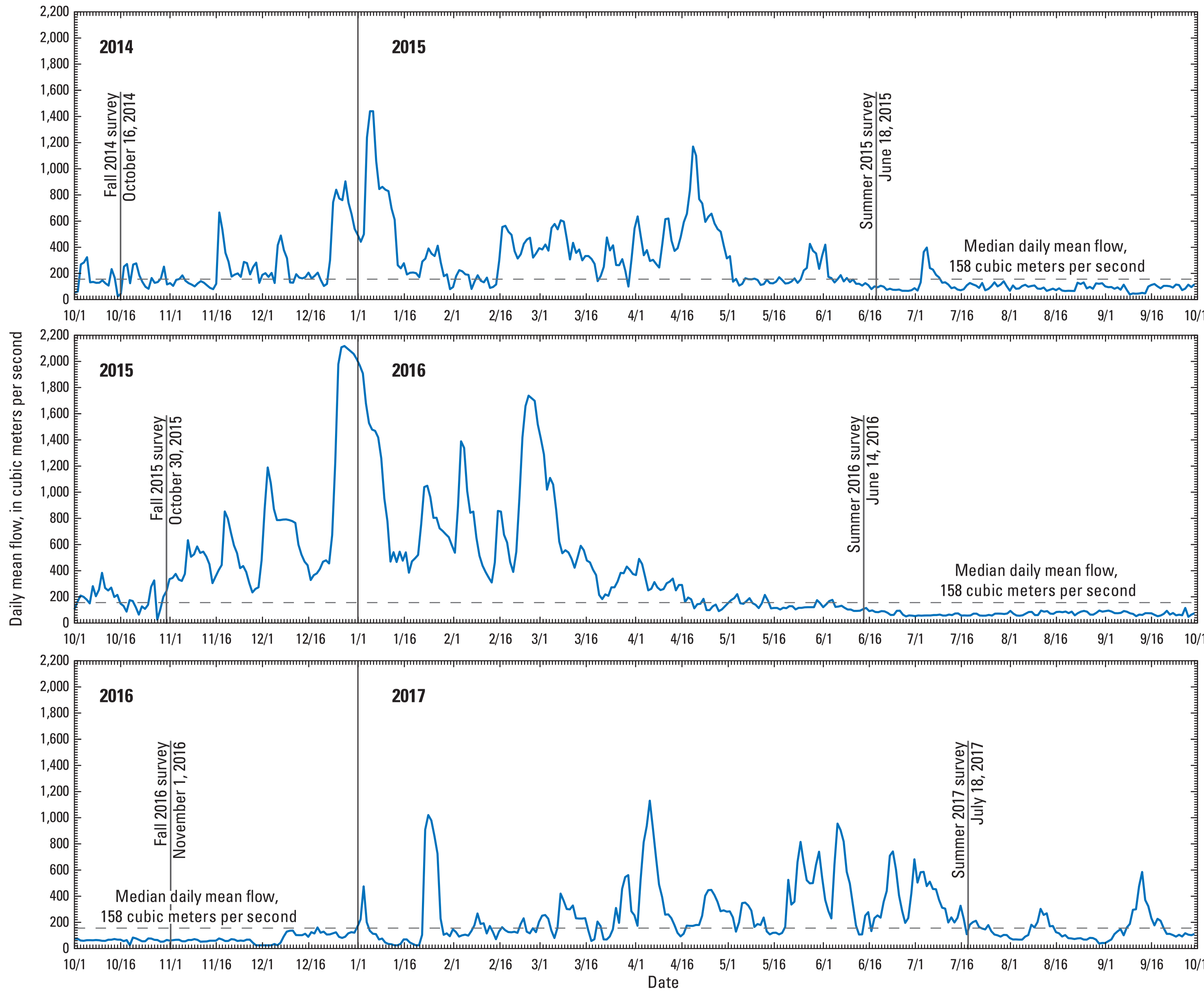

Figure 12. Daily mean flow on the Coosa River downstream from Logan Martin Dam near Vincent, Alabama, for October 1, 2014, to September 30, 2017, by water year, with survey dates indicated.

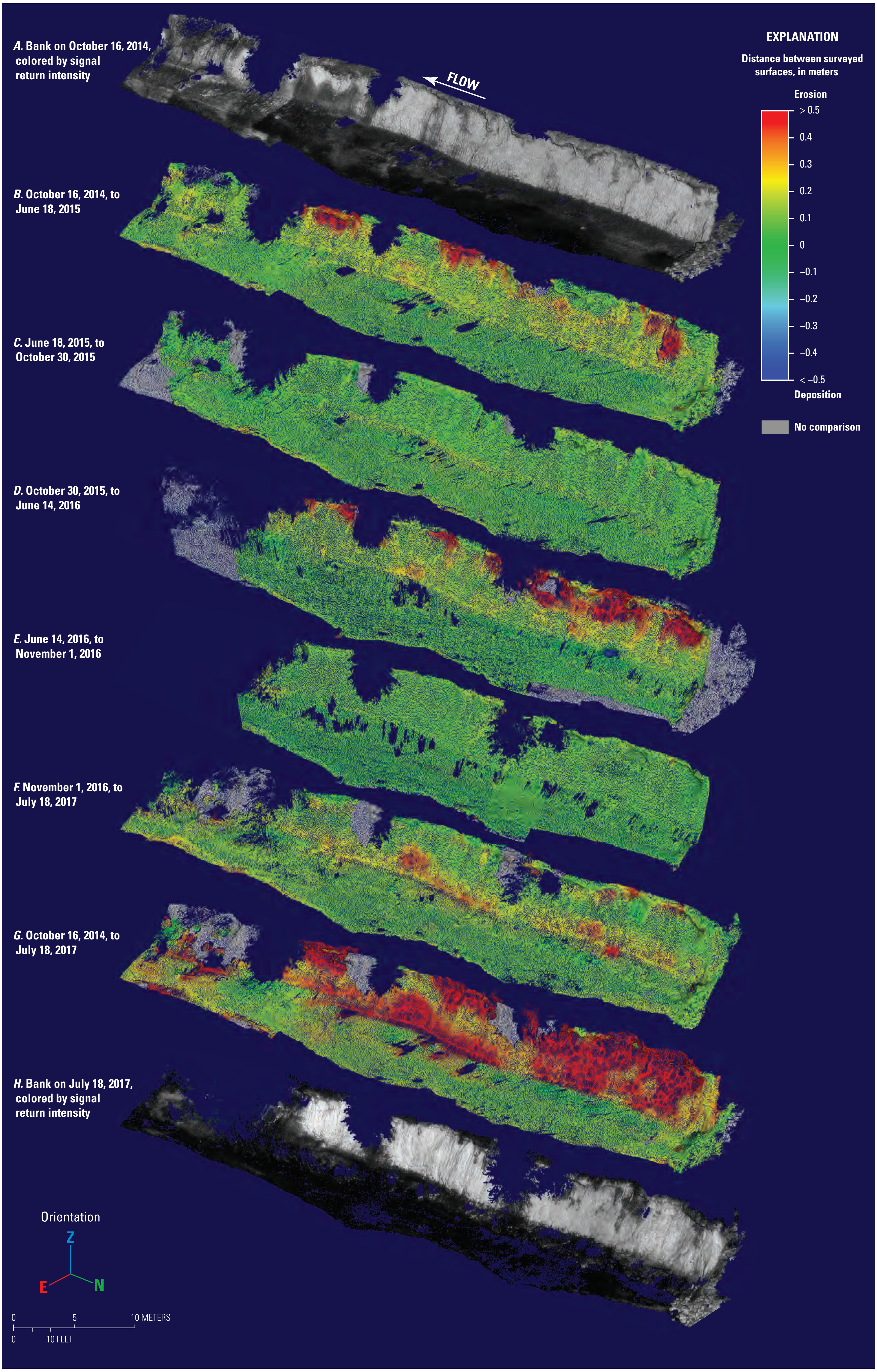

Figure 13. Surveyed banks and incremental differences between surveys at Logan Martin Dam site LM–102 on the Coosa River near Vincent, Alabama, for October 16, 2014, through July 18, 2017. *A*, bank on October 16, 2014, colored by signal return intensity; *B*, October 16, 2014, to June 18, 2015; *C*, June 18, 2015, to October 30, 2015; *D*, October 30, 2015, to June 14, 2016; *E*, June 14, 2016, to November 1, 2016; *F*, November 1, 2016, to July 18, 2017; *G*, October 16, 2014, to July 18, 2017; and *H*, bank on July 18, 2017, colored by signal return intensity.

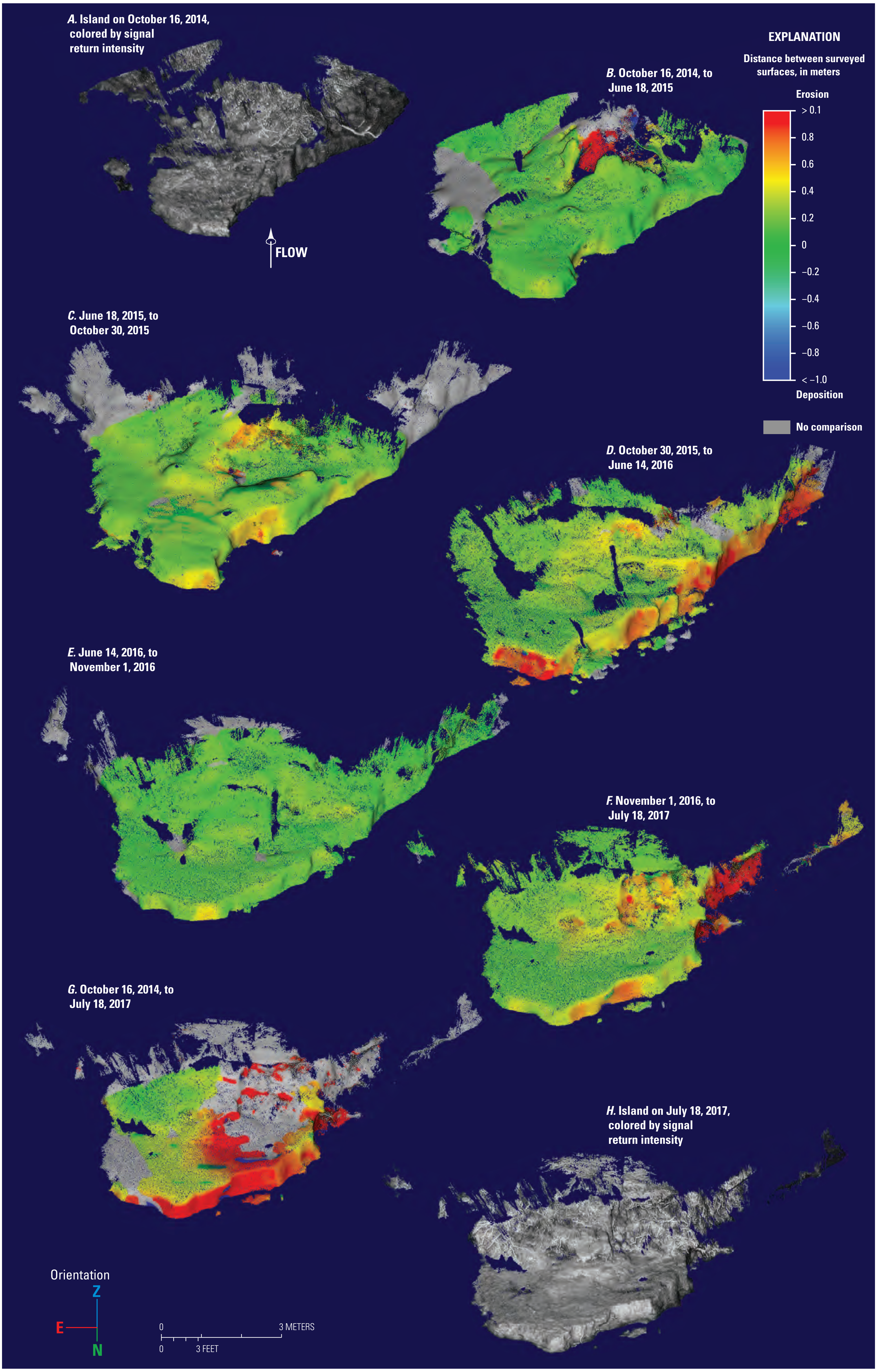

Figure 14. Surveyed banks and incremental differences between surveys at Logan Martin Dam site LM–108 on the Coosa River near Vincent, Alabama, for October 16, 2014, through July 18, 2017. *A*, island on October 16, 2014, colored by signal return intensity; *B*, October 16, 2014, to June 18, 2015; *C*, June 18, 2015, to October 30, 2015; *D*, October 30, 2015, to June 14, 2016; *E*, June 14, 2016, to November 1, 2016; *F*, November 1, 2016, to July 18, 2017; *G*, October 16, 2014, to July 18, 2017; and *H*, island on July 18, 2017, colored by signal return intensity.

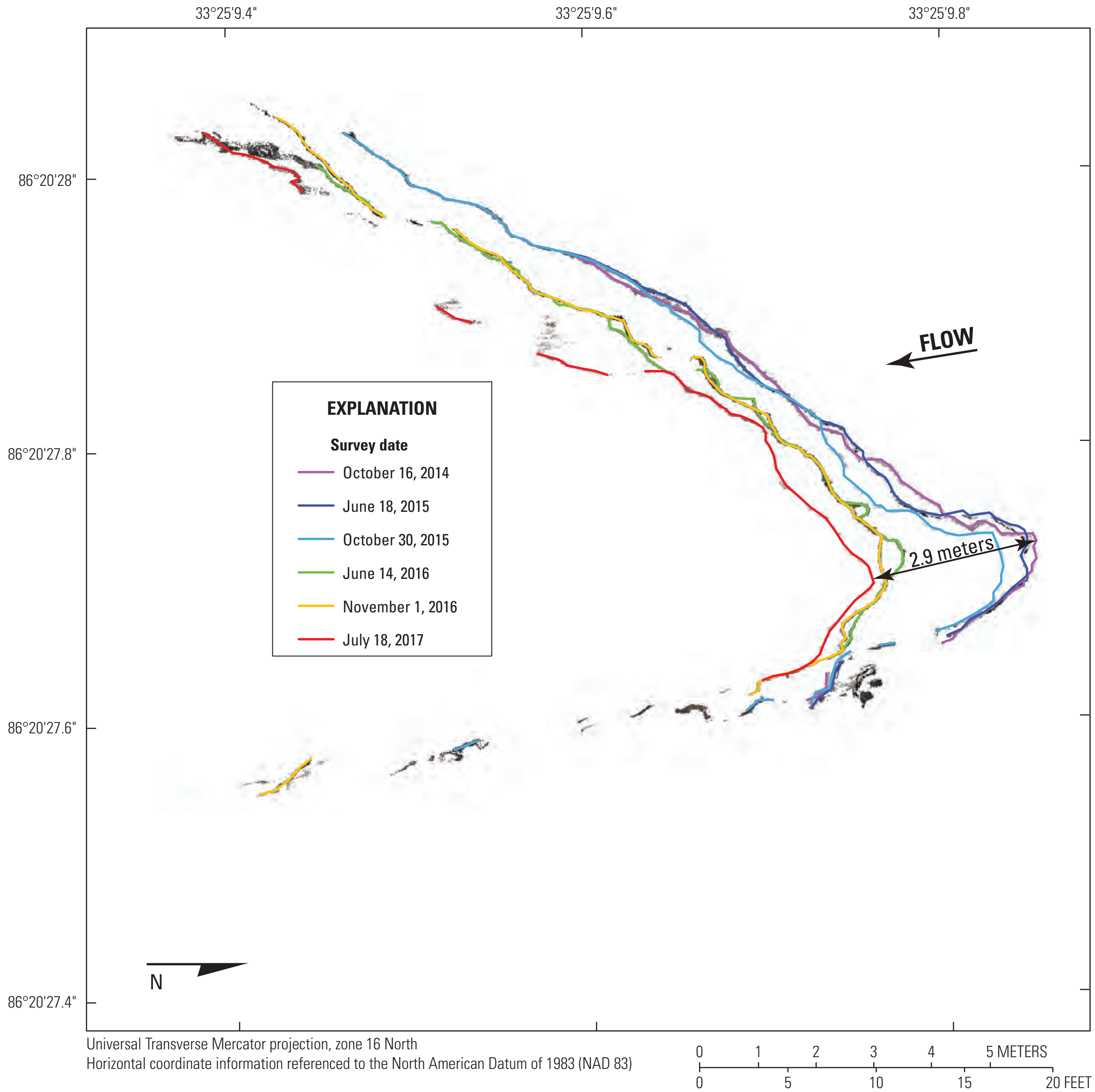

Figure 15. Surveyed points from a narrow band of data near the water line at Logan Martin Dam site LM–108 on the Coosa River near Vincent, Alabama, for October 16, 2014, through July 18, 2017.

Site WB–101

Comparison of the fall 2014 (November 2014) and summer 2017 (July 2017) T–lidar scans of site WB–101 indicated normalized erosion 0.331 m^3/m^2 during the study (table 3). The difference between the scans exceeded 0.5 m along much of the bank (fig. 17*G*).

Net erosion was observed during three of the five intervals between T–lidar scans, with the greatest amount of normalized erosion, 0.226 m^3/m^2, occurring between the fall 2015 (January 2016) and summer 2016 (July 2016) scans (table 3). Greater than 0.2 m of change was indicated for much of the bank, with some locations exceeding 0.5 m (fig. 17*D*). During the interval between the fall 2015 and summer 2016 scans, an extended period of above-median daily mean flows lasted through mid-April, 2016, with occasional above-median flows occurring from mid-April through mid-May 2016. From mid-May 2016 until the summer 2016 scan on July 11, 2016, daily mean flows were well below the median of 114 m^3/s (fig. 16). The maximum daily mean flow through Walter Bouldin Dam of 809 m^3/s, occurred on April 7, 2017. Furthermore, during the fall 2016 to summer 2017 interval, daily mean flows exceeded 700 m^3/s four times: April 4–8, June 6–8, June 23–25, and July 1, 2017 (fig. 16).

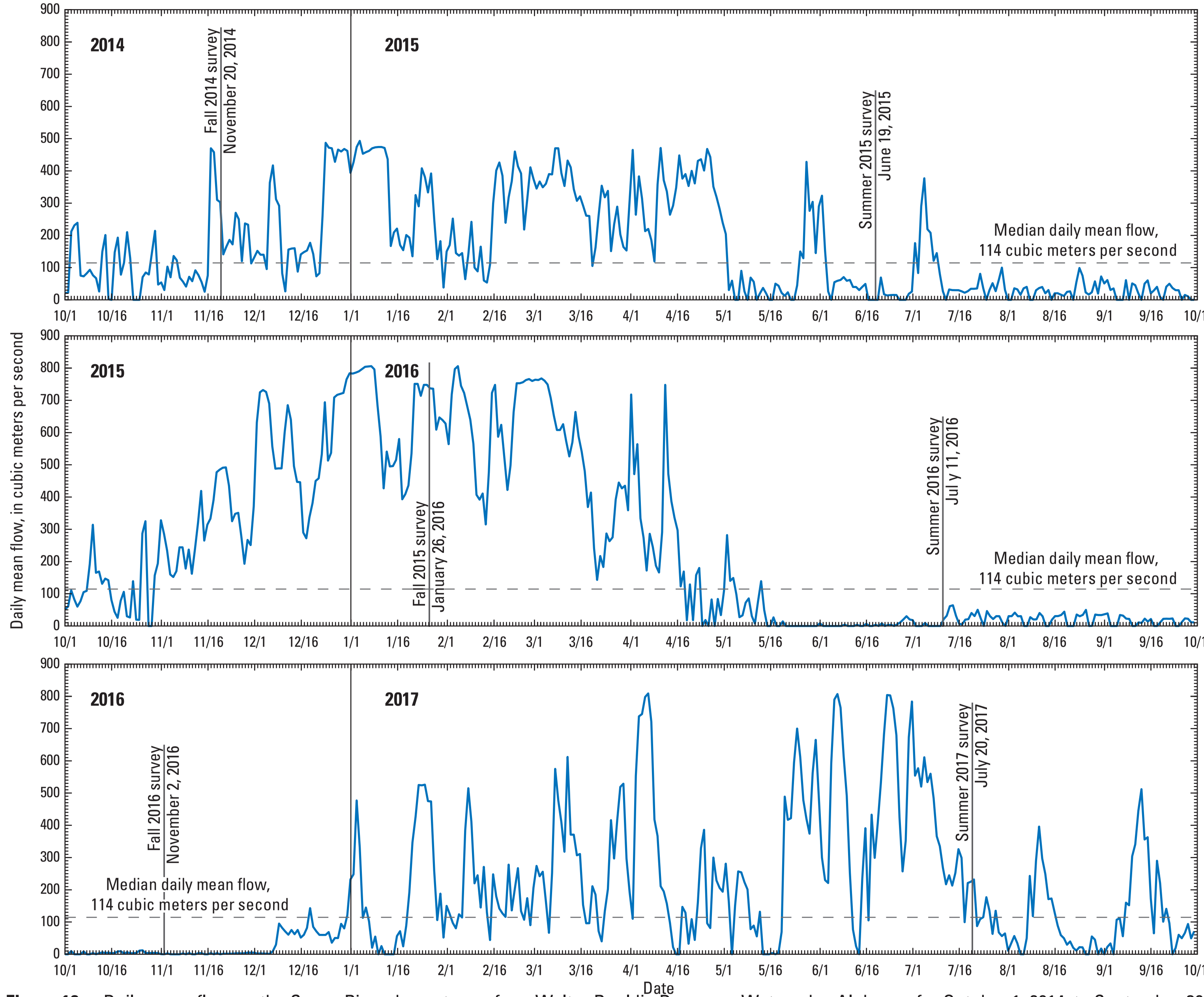

Figure 16. Daily mean flow on the Coosa River downstream from Walter Bouldin Dam near Wetumpka, Alabama, for October 1, 2014, to September 30, 2017, by water year, with survey dates indicated.

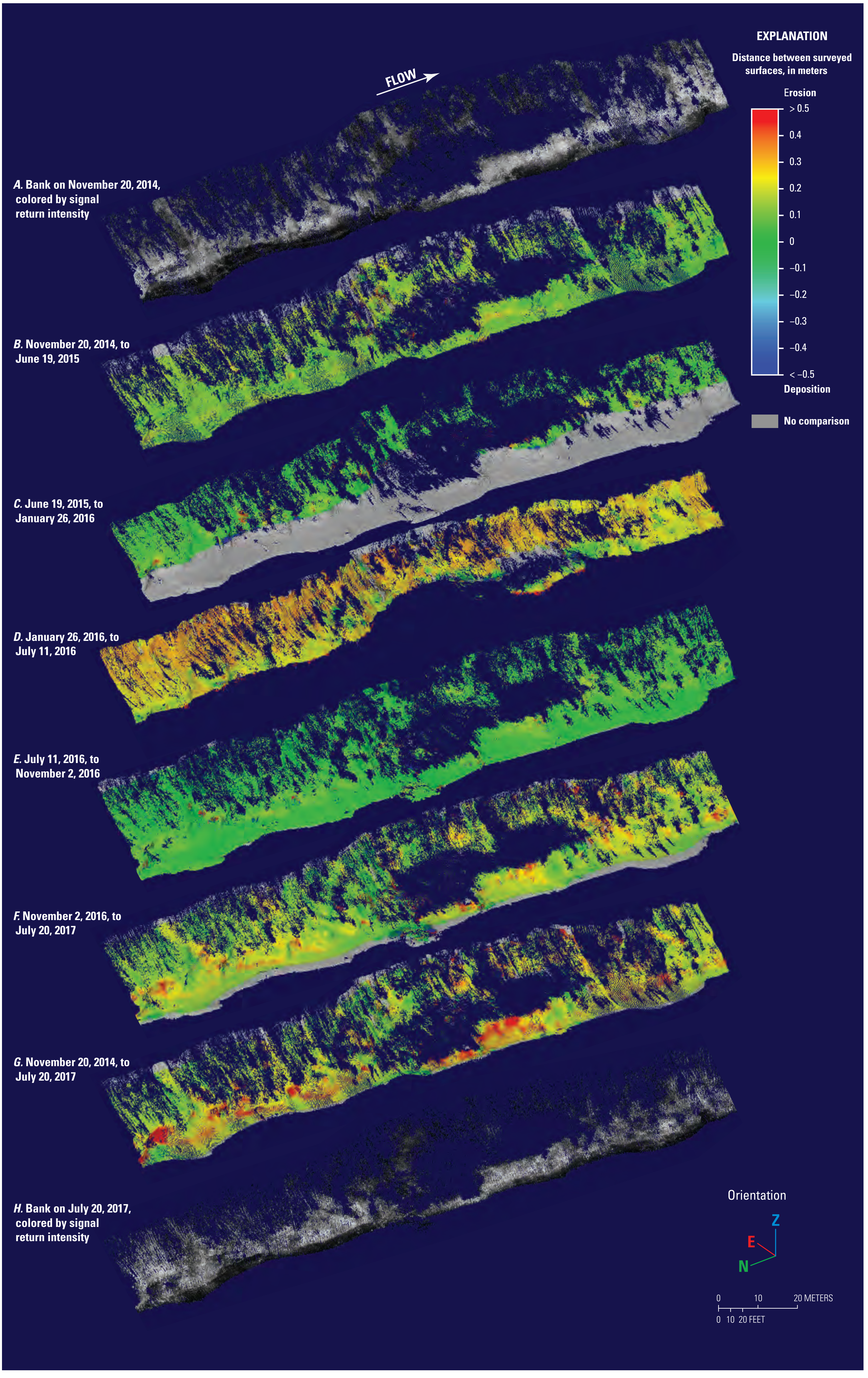

Figure 17. Surveyed banks and incremental differences between surveys at Walter Bouldin Dam site WB–101 on the Coosa River near Wetumpka, Alabama, for November 20, 2014, through July 20, 2017. *A*, bank on November 20, 2014, colored by signal return intensity; *B*, November 20, 2014, to June 19, 2015; *C*, June 19, 2015, to January 26, 2016; *D*, January 26, 2016, to July 11, 2016; *E*, July 11, 2016, to November 2, 2016; *F*, November 2, 2016, to July 20, 2017; *G*, November 20, 2014, to July 20, 2017; and *H*, bank on July 20, 2017, colored by signal return intensity.

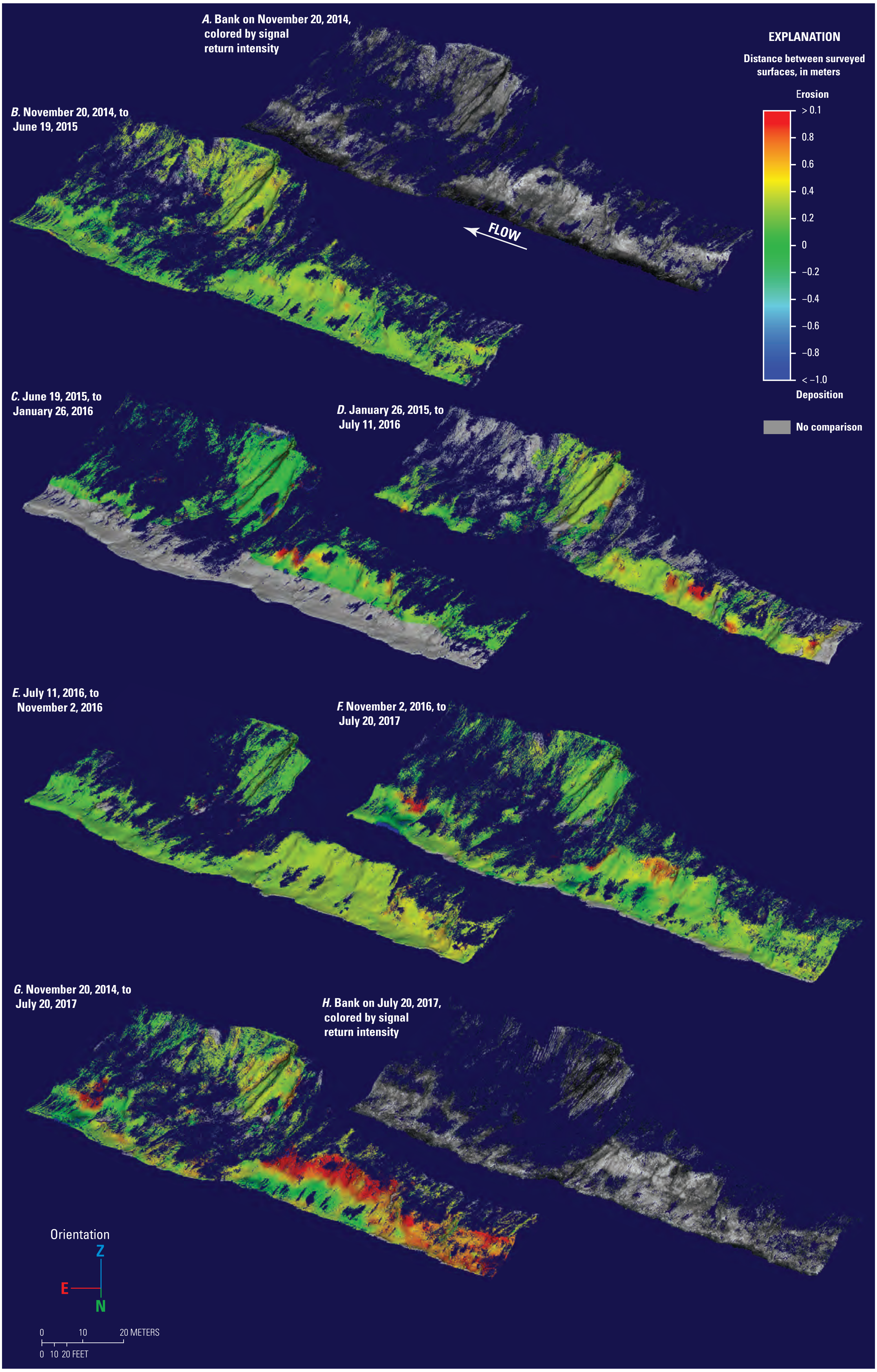

Figure 18. Surveyed banks and incremental differences between surveys at Walter Bouldin Dam site WB–106 on the Coosa River near Wetumpka, Alabama, for November 20, 2014, through July 20, 2017. *A*, bank on November 20, 2014, colored by signal return intensity; *B*, November 20, 2014, to June 19, 2015; *C*, June 19, 2015, to January 26, 2016; *D*, January 26, 2016, to July 11, 2016; *E*, July 11, 2016, to November 2, 2016; *F*, November 2, 2016, to July 20, 2017; *G*, November 20, 2014, to July 20, 2017; and *H*, bank on July 20, 2017, colored by signal return intensity.

Net deposition was observed between the summer and fall 2015 (June 2015 and January 2016) scans and between the summer and fall 2016 (July and November 2016) scans, with the greatest amount of normalized deposition, 0.196 m^3/m^2, occurring between the summer and fall 2016 scans (table 3). Relatively uniform change of about 0–0.2 m was observed for much of the bank during that interval (fig. 17*E*). Daily mean flows during the summer to fall 2016 period were below the median of 114 m^3/s (fig. 16).

Site WB–106

Comparison of the fall 2014 (November 2014) and summer 2017 (July 2017) T–lidar scans of site WB–106 indicated normalized erosion 0.467 m^3/m^2 during the study (table 3). The difference between the scans exceeded 1.0 m along much of the upstream half of the bank and within a distance of about 20 m from the waterline (fig. 18*G*).

Net erosion was observed during three of the five intervals between T–lidar scans, with the greatest amount of normalized erosion, 0.457 m^3/m^2, occurring between the summer 2016 (July 2016) and fall 2016 (November 2016) scans (table 3). Although there are no “hot-spots” of erosion during this period, comparison of the scans indicated that the greatest amount of change occurred near the upstream end of the bank (fig. 18*E*). During the interval between the summer and fall 2016 scans, daily mean flows were below the median of 114 m^3/s (fig. 16), which is anomalous. Assessment of erosion during this interval was likely biased by abundant vegetation present during the summer 2016 scan, which obscured the bank and resulted in a smaller surface area that could be surveyed compared with the fall 2016 scan.

Similar amounts of erosion were observed during the intervals between the fall 2014 to summer 2015 and fall 2016 to summer 2017 scans; normalized erosion was 0.084 and 0.083 m, respectively (table 3). Although erosion seems to be mostly minor and distributed somewhat uniformly throughout the bank in both intervals, in the comparison of the fall 2016 to summer 2017 scans, greater than 0.6 m of change was observed at several locations on the bank within about 20 m of the waterline (fig. 18*F*). Daily mean flows through Walter Bouldin Dam during the fall 2016 to summer 2017 interval were below the median of 114 m^3/s during the month of November 2016 and were mostly above the median for the remainder of the interval (fig. 16). The maximum daily mean flow experienced during the study, 809 m^3/s, occurred on April 7, 2017, during the fall 2016 to summer 2017 interval, and daily mean flows exceeded 700 m^3/s four times during the interval: April 4–8, June 6–8, June 23–25, and July 1, 2017 (fig. 16).

Net deposition was observed between the summer and fall 2015 (June 2015 and January 2016) scans and between the fall 2015 and summer 2016 (January and July 2016) scans, with the greatest amount of normalized deposition, 0.121 m^3/m^2, occurring between the summer and fall 2015 scans (table 3). Relatively minor, uniform change of less than about 0.2 m was observed between the scans, although one area in the middle of the bank about 20 m from the waterline experienced greater than 0.6 m of erosion (fig. 18*C*). Daily mean flows during the summer to fall 2015 interval were mostly below the median of 114 m^3/s from June through October 2015 and above the median and generally increasing from November to January 26, 2016, the date of the fall 2015 scan (fig. 16). In fact, daily mean flows exceeded 700 m^3/s three times immediately before the fall 2015 scan: December 3–6, 2015; December 27, 2015, to January 9, 2016; and January 22–26, 2016.

General Findings and Implications

Results from T–lidar scan comparisons indicate that intervals between scans that exhibited the greatest amounts of normalized erosion generally corresponded to periods of above-median flow, and intervals between scans that exhibited the least amounts of erosion—or deposition—corresponded to periods of below-median flow. Of the five intervals between scans, the three that exhibited the greatest amounts of normalized erosion corresponded to periods of above-median flow through the dams (table 3; figs. 6, 9, 12, 16). With the exception of site WB–106, erosion was observed at all six sites during the three “Fall to Summer” intervals, and, with the additional exception of site NH–104, the greatest amounts of erosion occurred during either the fall 2015 to summer 2016 or fall 2016 to summer 2017 interval. However, the interval that experienced the greatest daily mean flows, fall 2015 to summer 2016, did not correspond to the greatest amounts of erosion at all sites. Site WB–106 was surveyed on January 26, 2016, in the middle of an extended period of very high flow through Walter Bouldin Dam that lasted from mid-December 2015 to mid-April 2016 (fig. 16). In mid-May 2016, flows through the dam abruptly went to zero or near-zero until the date of the next survey on July 11, 2016 (fig. 16). The shift from high- to low-flow was not as drastic at H Neely Henry or Logan Martin Dams (figs. 9, 12), and was the result of a drought on the Coosa River that necessitated all flow into Jordan Lake being diverted through Jordan Dam for habitat preservation. The abrupt shift from relatively high flows to essentially zero flow at Walter Bouldin Dam may explain why deposition occurred at site WB–106 during the fall 2015 to summer 2016 interval, as material sloughed from the banks due to excess pore pressure but was not carried away by higher flows, whereas erosion occurred at all other sites for this interval.

Intervals between scans that exhibited the least amounts of normalized erosion generally corresponded to periods of below-median flow through the dams (table 3; figs. 6, 9, 12, 16). With the exception of sites NH–104 and WB–106, the summer 2015 to fall 2015 or summer 2016 to fall 2016 intervals exhibited the least amounts of normalized erosion or minor amounts of deposition. Mid-June through mid-October 2015 was a period of generally below-median flow through the dams, with few daily mean flows exceeding 275 m^3/s (figs. 9, 12, 16). After November 1, 2015, flows through all three dams increased to above-median values through January 2016, with the largest flows experienced during the study occurring at all three dams in late December 2015 (figs. 9, 12, 16). Site NH–104 was surveyed on December 10, 2015, 1 week after a relatively sharp rise in daily mean flow from 265 m^3/s on November 30 to 1,000 m^3/s on December 3. This may explain the large amount of net erosion observed for site NH–104 relative to the other sites during the summer 2015 to fall 2015 interval. Sites WB–101 and WB–106 experienced minor to moderate normalized deposition during the same interval, while sites LM–102 and LM–108 experienced minor normalized erosion. Furthermore, the dates that the T–lidar scans were conducted likely account for the variation between sites. The fall 2015 scans of sites WB–101 and WB–106 were conducted on January 26, 2016, after a sustained period of above-median flows and 3 weeks after daily mean flows had peaked at greater than 800 m^3/s on January 5; conversely, scans of sites LM–102 and LM–108 were conducted on October 30, 2015, 1 month after daily mean flows through Logan Martin Dam had increased slightly after about 3 months of mostly below-median flow.

The total surface area available to be surveyed during a given survey had an effect on the comparison results. During the summer 2016 to fall 2016 interval, an anomalously large amount of normalized erosion was observed at site WB–106, while four of the five other sites experienced minor to moderate deposition, and site LM–102 experienced a minor amount of erosion (table 3). The amount of erosion observed during the summer 2016 to fall 2016 interval—and consequently for the duration of the study—at site WB–106 may be biased high because of the relatively smaller surface area that could be surveyed on the date of the summer 2016 scan (July 11, 2016) resulting from dense vegetation obscuring the upper banks (fig. 18*E*). Furthermore, the fall 2015 surveys at the H Neely Henry and Walter Bouldin Dam sites were affected by above-median flows (figs. 9, 16), which caused the lower part of the surveyed bank to be inundated, limiting the area that could be surveyed and used for comparison. This reduction in area may have skewed the comparison results, creating more apparent deposition (or less erosion) during the summer 2015 to fall 2015 interval and more apparent erosion during the fall 2015 to spring 2016 interval. While none are currently planned, future surveys could benefit from deliberate attempts to survey during leaf-off and low-flow conditions to minimize the effects of vegetation and inundation.

During the study, site LM–108, the island in the middle of the Coosa River downstream from Logan Martin Dam, exhibited the largest normalized erosion of all six sites (table 3; figs. 14, 15). The normalized erosion during the study period, 2.05 m^3/m^2, was more than four times that of the site with the next greatest amount (site WB–106, 0.467 m^3/m^2; table 3), and likely is because LM–108 experiences head-on flow as compared with predominantly shear flow at the other sites. The overall retreat of the bank at the upstream end of the island near the water line is estimated at 2.9 m (fig. 15). Most of this retreat seems to have occurred during the fall 2015 to summer 2016 interval (fig. 15; table 3), during the period of the largest flows at this site (fig. 13).

Summary and Conclusions

The Alabama Power Company operates a series of dams on the Coosa River in east central Alabama. Seven dams impound the river to form six reservoirs: Weiss Lake, Neely Henry Lake, Logan Martin Lake, Lay Lake, Lake Mitchell, and Lake Jordan. Streamflow below these reservoirs primarily is controlled by power generation at the dams, and there is ongoing concern about the stability of selected stream banks downstream from the dams. As part of the Federal Energy Regulatory Commission relicensure of the Coosa River project in the early 2000s, the Alabama Power Company and various stakeholders identified particular areas of concern to monitor and document the extent of erosion. From 2014 to 2017, the U.S. Geological Survey, in cooperation with the Alabama Power Company, conducted a monitoring program of the geomorphic conditions of six selected reaches along the Coosa River downstream from H Neely Henry Dam near Gadsden, Logan Martin Dam near Vincent, and Walter Bouldin Dam near Wetumpka, Alabama, using boat- and tripod-mounted terrestrial light detection and ranging (T–lidar) technology. The results of the investigation served to help the Alabama Power Company evaluate effects on the stream channel geomorphology. This report documents the results of the periodic stream bank surveys, equipment and methods used and differences between surveys, which were used to compute volumes of material eroded or deposited. Erosion and deposition were then correlated to streamflow conditions between surveys.

Results of the comparisons of T–lidar scans indicated that intervals between scans that exhibited the greatest amounts of erosion generally corresponded to periods of above-median flow, and that intervals between scans that exhibited the least amounts of erosion, or deposition, generally corresponded to periods of below-median flow. During the summer 2016 to fall 2016 interval, an anomalously large amount of erosion was observed at site WB–106 downstream from Walter Bouldin Dam near Wetumpka, Alabama. The amounts of erosion observed during the interval, and consequently for the duration of the study, at site WB–106 may be biased high because of the relatively smaller surface area that could be surveyed on the date of the summer 2016 scan (July 11, 2016) resulting from dense vegetation obscuring the upper banks during the survey. Apparent deposition or additional erosion may also have been caused by inundation during one of the survey intervals. This suggests that, in future investigations using T–lidar technology, it may be preferable to conduct scans during periods of leaf-off and low flow to avoid bias introduced by parts of the banks of interest being inundated or obscured by vegetation.

During the study, site LM–108, an island in the middle of the Coosa River downstream from Logan Martin Dam, exhibited normalized erosion of 2.05 cubic meters per square meter of area, the greatest amount of all six sites, likely because this site experiences head-on flow from the river. Bank retreat at the upstream end of the island near the waterline was estimated at 2.9 meters. The remaining five reaches were exposed to shear flow from the river, with the greatest amount of normalize erosion, 0.467 cubic meter per square meter of area, being exhibited by site WB–106, on the right bank downstream from Walter Bouldin Dam.

References Cited

Applanix Corporation, 2009, POS–Pac™ MMS™ GNSS-inertial tools user guide, rev. 4: Richmond Hill, Ontario, Canada, PUBS–MAN–001768, 523 p.

Byrnes, M.R., Baker, J.L., and Li, F., 2002, Quantifying potential measurement errors and uncertainties associated with bathymetric change analysis: Vicksburg, Miss., U.S. Army Corps of Engineers, ERDC/CHL CHETN–IV–50, 17 p., accessed September 26, 2018, at http://www.dtic.mil/dtic/tr/fulltext/u2/a588888.pdf.

CloudCompare, 2018, CloudCompare—User manual (ver. 2.6.1): CloudCompare, accessed September 25, 2018, at http://cloudcompare.org/doc/qCC/CloudCompare%20v2.6.1%20-%20User%20manual.pdf.

Collins, B.D., Kayen, R., Minasian, D., and Reiss, T., 2009, Terrestrial lidar datasets of New Orleans, Louisiana, levee failures from Hurricane Katrina, August 29, 2005: U.S. Geological Survey Data Series 470, 24 p. [Also available at https://pubs.usgs.gov/ds/470/ds470.pdf.]

Collins, B.D., Kayen, R., Reiss, T., and Sitar, N., 2007, Terrestrial LIDAR investigation of the December 2003 and January 2007 activations of the Northridge Bluff Landslide, Daly City, California: U.S. Geological Survey Open-File Report 2007–1079, 32 p. [Also available at https://doi.org/10.3133/ofr20071079.]

Evans, C.M., 1999, The complete guide to Alabama weather: Birmingham, Ala., Seacoast Publishing, 112 p.

FARO Technologies, Inc., 2014, FARO Laser Scanner Focus^{3D} X 130 manual: Lake Mary, Fla., FARO Technologies, Inc., 118 p. [Also available at https://faro.app.box.com/s/r45cyjqengcts8vnh5kawemgsvdfxt81.]

FARO Technologies, Inc., 2016, SCENE 6.2 user manual: Lake Mary, Fla., FARO Technologies, Inc., 396 p. [Also available at https://faro.app.box.com/s/uivkgf3jyrxcxn5ofazlohjnadddknhr/folder/51145992789.]

Huizinga, R.J., and Wagner, D.M., 2019, Erosion monitoring along the Coosa River, Alabama, using terrestrial light detection and ranging (T–LiDAR) technology, 2014–2017: U.S. Geological Survey data release, https://doi.org/10.5066/F7GF0SS8.

Innovmetric, 2012, Parametric Image Format: Polyworks/IMView software, accessed February 12, 2012, at http://www.innovmetric.com/polyworks/3D-scanners/viewer.aspx?lang=en.

Kimbrow, D.R., and Lee, K.G., 2013, Erosion monitoring along the Coosa River below Logan Martin Dam near Vincent, Alabama, using terrestrial light detection and ranging (T–LiDAR) technology: U.S. Geological Survey Scientific Investigations Report 2013–5128, 7 p. [Also available at https://doi.org/10.3133/sir20135128.]

Lague, D., Brodu, N., and Leroux, J., 2013, Accurate 3D comparison of complex topography with terrestrial laser scanner—Application to the Rangitikei canyon, New Zealand: Geosciences Rennes, 28 p., accessed September 25, 2018, at https://arxiv.org/ftp/arxiv/papers/1302/1302.1183.pdf.

Stock, G.M., Bawden, G., Green, J., Hanson, E., Downing, G., Collins, B., Bond, S., and Leslar, M., 2011, High resolution three-dimensional imaging and analysis of rock falls in Yosemite Valley, California: Geosphere, v. 7, no. 2, p. 573–581. [Also available at https://doi.org/10.1130/GES00617.1.]

Teledyne-Optech, 2012, ILRIS laser scanner operation manual: Vaughan, Ontario, Canada, Teledyne-Optech, Inc., Issue 0040170/Rev G., 288 p.

For more information about this publication, contact:
Director, USGS Central Midwest Water Science Center
1400 Independence Road
Rolla, MO 65401
573–308–3667

For additional information, visit: https://www.usgs.gov/centers/cm-water

Publishing support provided by the
Rolla Publishing Service Center

USGS

Huizinga and Wagner—**Erosion Monitoring Along Bank Locations of the Coosa River Using Terrestrial Light Detection and Ranging Technology**—SIR 2019–5023

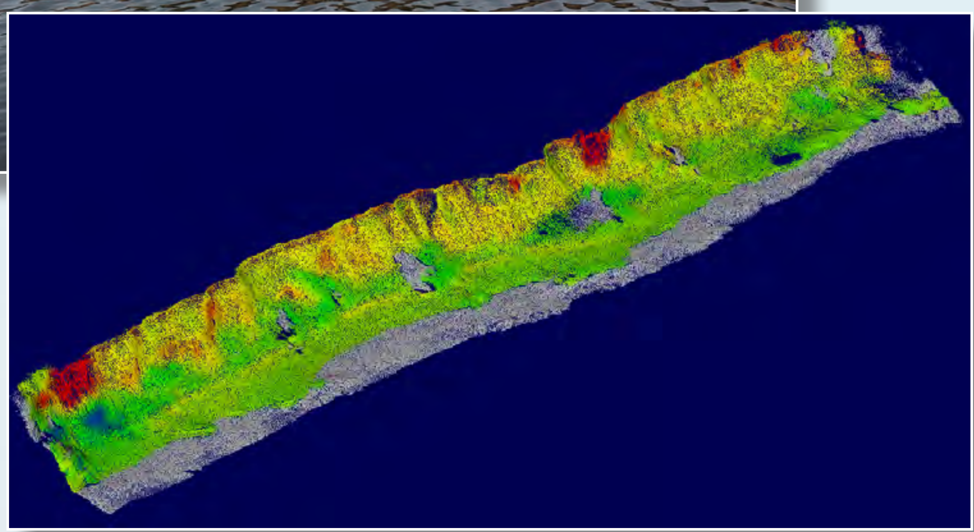

ISSN 2328-0328 (online)
https://doi.org/10.3133/sir20195023